EXPERIMENTAL INVESTIGATION OF AN RC EXTERIOR BEAM-COLUMN JOINT BEHAVIOR STRENGTHENED WITH FRP

by

Md. Kudrat-E-Jahan

MASTER OF ENGINEERING IN CIVIL ENGINEERING (STRUCTURAL)

DEPARTMENT OF CIVIL ENGINEERING

BANGLADESH UNIVERSITY OF ENGINEERING AND TECHNOLOGY

March, 2016

EXPERIMENTAL INVESTIGATION OF AN RC EXTERIOR BEAM-COLUMN JOINT BEHAVIOR STRENGTHENED WITH FRP

by

Md. Kudrat-E-Jahan

Submitted to the Department of Civil Engineering, Bangladesh University of Engineering and Technology (BUET), Dhaka in partial fulfillment of the requirements for the degree of

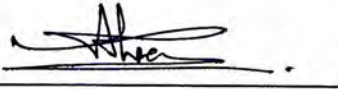**MASTER OF ENGINEERING IN CIVIL ENGNEERING (STRUCTURAL)**

DEPARTMENT OF CIVIL ENGINEERING

BANGLADESH UNIVERSITY OF ENGINEERING AND TECHNOLOGY

March, 2016

This thesis titled "**Experimental Investigation of an RC Exterior Beam-Column Joint Behavior Strengthened with FRP**", submitted by Md. Kudrat-E-Jahan, Roll No. 0409042376P, Session: April 2009, has been accepted as satisfactory in partial fulfillment of the requirement for the degree of **Master of Engineering in Civil Engineering (Structural)** on 05th March, 2016.

BOARD OF EXAMINERS

Dr. Raquib Ahsan   **Chairman**
Professor   (Supervisor)
Department of Civil Engineering, BUET

Dr. Syed Ishtiaq Ahmed   **Member**
Professor
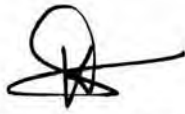Department of Civil Engineering, BUET

Dr. Mohammad Al Amin Siddique   **Member**
Associate Professor
Department of Civil Engineering, BUET

DECLARATION

It is hereby declared that, except where specific references are made, the work embodied in this thesis is the result of investigation carried out by the author under the supervision of Dr. Raquib Ahsan, Professor, Department of Civil Engineering, BUET.

Neither the thesis nor any part of it is concurrently submitted elsewhere for the award of any degree or diploma.

_____

(Md. Kudrat-E-Jahan)

DEDICATED TO

MY PARENTS, TEACHERS AND FAMILY

ACKNOWLEDGEMENT

ABSTRACT

Beam Column joints experience large shear forces during seismic events and may undergo brittle failure which is not preferred. Eminent scholars suggested different technologies and methods to strengthen the beam column joints. FRPs, which have high strength to weight ratio, are also suggested as retrofitting materials for strengthening RC structural members. From literature review, it is found that FRPs are very effective in strengthening the shear, flexural and axial capacities of beams and columns. They are being effectively used for retrofitting exterior and corner joints due to ease of accessibility and placement.

This experimental study is under taken to study the behavior of RC exterior beam-column joints which lack in shear reinforcement and strengthened by FRPs. Total three models have been prepared of which one joints have been strengthened by Carbon FRP (CFRP) Fabrics and remaining two was control specimens with tie and without tie at joints. The samples have been subjected to incremental cyclic loading provided by hydraulic jacks under constant axial or gravity load and their load-deformation behaviors have been measured by dial gauges and video extensometer. The behavior of the strengthened joint are compared with the control model.

The joints without shear reinforcement undergo brittle failure under cyclic loading. But their ductility increases with increased concrete strength. The joints strengthened by the CFRPs show better load bearing capacity with enhanced ductile behavior.

TABLE OF CONTENTS

LIST OF FIGURES

LIST OF TABLES

NOTATIONS AND SYMBOLS

A_g = Gross area of section

Aj = Effective area of the joint

A_s = Area of non pre-stressed steel reinforcement

A_{sh} = Total cross sectional area of the transverse reinforcement (including cross ties) within spacing s and perpendicular to dimension h_c

A_{st} = Total area of longitudinal reinforcement

b = Width of rectangular cross section

b_c = Effective width of the column

b_b = Effective width of the beam

b_j = Effective width of the beam column joint

B'_s = Bond force contribution from top reinforcement

b_w = Web width or diameter of circular section

c = Distance from extreme compression fiber to the neutral axis

C_b = Compressive force acting on beam reinforcement

C'_s = Compression force developed in the top bars

C_E = Environmental-reduction factor

C_f = Diagonal compressive force

C_{ult} = Ultimate compressive force

d = Distance from extreme compression fiber to the neutral axis

d_f = Depth of FRP shear reinforcement

E_c = Modulus of elasticity of concrete

E_f = Tensile modulus of elasticity of FRP

E_s = Modulus of elasticity of steel

f_c = Compressive stress in concrete

f'_c = Specified compressive strength of concrete, psi /MPa

f_f = Stress level in the FRP reinforcement

$f_{f,s}$ = Stress level in the FRP caused by a moment within the elastic range

f_{fe} = Effective stress in the FRP; stress level attained at section failure

f^*_{fu} = Ultimate tensile strength of the FRP material as reported by the manufacturer

f_{fu} = Design ultimate tensile strength of FRP

f_y	=	Specified yield strength of non pre-stressed steel reinforcement
h	=	Overall thickness of a member,
h_c	=	Depth of column
h_j	=	Depth of the beam column joint
k	=	Ratio of the depth of the neutral axis to the reinforcement depth measured on the same side of neutral axis
k_f	=	Stiffness per unit width per ply of the FRP reinforcement, $k_f = E_f\, t_f$
k_1	=	Modification factor applied to k_v to account for the concrete strength
k_2	=	Modification factor applied to $_{kv}$ to account for the wrapping scheme
L_e	=	Active bond length of FRP laminate
l_c	=	Height of the story
l_{df}	=	Development length of FRP system
M_p	=	Plastics moment capacity
M_s	=	Sagging Moment
n	=	Number of plies of FRP reinforcement
s	=	Spacing of the transverse reinforcement
t_f	=	Nominal thickness of one ply of the FRP reinforcement
T_f	=	Tensile force from the slab reinforcement
T_g	=	Glass-transition temperature, °F (°C)
T_b	=	Tensile force acting on the beam reinforcement
T_{ult}	=	Ultimate Tensile force
V_b	=	Vertical beam shear
V_{col}	=	Column shear force
V_n	=	Nominal shear strength
V_s	=	Nominal shear strength provided by steel stirrups
V_f	=	Nominal shear strength provided by FRP stirrups
V_{jh}	=	Horizontal shear force within joint core
w_f	=	Width of the FRP reinforcing plies, in. (mm)
Z_b	=	Lever arm of beam tensile and compressive force
α	=	Angle of inclination of stirrups or spirals, degrees
β	=	Ratio of the bottom reinforcement to top reinforcement
Δ_y	=	Yield deflection
Δ_u	=	Ultimate deflection

ε_f = Strain level in the FRP reinforcement, in./in. (mm/mm)

ε_{fe} = Effective strain level in FRP reinforcement, in./in. (mm/mm)

ε_{fu} = design rupture strain of FRP reinforcement, in./in.(mm/mm)

θ_y = Yield rotation

θ_u = Ultimate rotation

Φ = Strength reduction factor

γ = Factor used to express the stress level in the reinforcing bars

k_a = Efficiency factor for FRP reinforcement (based on the section geometry)

k_m = Bond-dependent coefficient for flexure

k_v = Bond-dependent coefficient for shear

ρ_f = FRP reinforcement ratio

ρ_g = Gross reinforcement ratio

ρ_s = Ratio of non pre-stressed reinforcement

ψ_f = Additional FRP strength-reduction factor

CHAPTER ONE
INTRODUCTION

1.1 Background

Recent earthquakes worldwide have illustrated the vulnerability of existing reinforced concrete (RC) beam-column joints to seismic loading. Poorly detailed joints, especially exterior ones, have been identified as critical structural elements, which appear to fail prematurely, thus performing as ''weak links'' in RC frames. A typical failure mode in poorly designed joints (lacking adequate transverse reinforcement) is concrete shear in the form of diagonal tension.

Reinforced concrete buildings constructed before 1970's were designed for gravity loads only and did not show adequate seismic performances (Bai 2003, Sharma et al. 2010). Weaknesses in joints were identified as one of the main causes for poor seismic performance. Forces induced by large lateral loads are different than that of the gravity loads. As the buildings and structures were not designed for lateral loads, many of them collapsed without warning to inhabitants causing numerous deaths. Mexico City experienced a great earthquake in 1985 where thousands of buildings were totally or partially collapsed making several thousand death tolls. Since then, considerable amounts of researches have been devoted to identify the details of the non-seismic designed buildings and methods to strengthen those (Murat et al. 2005). Most of the studies reasoned poor design and poor detailing of beam-column joints which may lead to a total or partial collapse of the buildings (Sezen 2012, Prota et al. 2004).

Strengthening of RC joints is a challenging task that poses major practical difficulties. A variety of techniques applicable to concrete elements have also been applied to joints with the most common ones being the construction of RC or steel jackets (Alcocer and Jirsa 1993). Reinforced concrete jackets and some forms of steel jackets, namely steel ''cages,'' require intensive labor and artful detailing. Moreover, concrete jackets increase the dimensions and weight of structural elements. Plain or corrugated steel plates have also been tried (Beres et al. 1992; Ghobarah et al. 1997). In addition to corrosion protection, these elements require special attachment through the use of either epoxy adhesives combined with bolts or special grouting.

More than two decade ago, a new technique for strengthening structural elements emerged. FRP materials, which are available today in the form of strips or in situ resin impregnated sheets, are being used to strengthen a variety of RC elements, including beams, slabs, columns, and shear walls, to enhance the flexural, shear, and axial capacity of such elements.

In a Reinforced Concrete (RC) building subjected to lateral loads such as earthquake and wind pressure, the beam-column joints has to dissipate large amount of energy. In existing frames, an easy and practical way to dissipate this energy coming from seismic or wind loading without a significant loss of, strength, stiffness and ductility is the use a Fiber Reinforced Polymer (FRP) retrofitting system. In the case of damaged buildings, this can be achieved through an FRP repairing system.

Shear failure at the joints is brittle in nature and not desirable. Thus the joints should be strengthened to move the failure to the beams. Such failure would be the best result for seismic upgrade and this means that very efficient ductile and energy dissipating mechanism is achieved which would maintain global integrity of the structure (Prota et al. 2004). As it is said that the structural ductility comes from the member ductility and member ductility is gained through the inelastic rotations. In RC members, inelastic rotation spread over definite regions called plastic hinges. Material properties are beyond elastic range therefore damage is obvious in inelastic deformations. In seismic design, it is desired that the plastic hinges should occur at beams rather than in the columns (FEMA 273, Akguzel et al. 2007). It leads to the Strong Column-Weak Beam Strategy which can be achieved by proper detailing in beams and at the joints. On the other hand, functional requirement of a joint, which is the zone of intersection of beam and columns, is to enable the adjoining members to develop and sustain their ultimate capacity. The joints should have adequate strength and stiffness to sustain the forces induced by the adjoining members.

1.2   Justification of the Study

In the last four decades, several research papers have been published on the effect of seismic loads on poorly detailed reinforced concrete beam-column joints, typical of pre-seismic code designed moment resisting frames. Cheung et al. (1993), Hakuto et al. (2000), Hwang and Lee (2000), Baglin and Scott (2000) are some of the important contributions. The research papers, however, on FRP repaired/upgraded beam-column

joints are limited. Antonopoulous and Triantafillou (2003) conducted a comprehensive experimental program through 2/3-scale testing of 18 exterior joints. Their study demonstrated the role of various parameters, e.g. area fraction of FRP, distribution of FRP etc, on shear strength of exterior joints. They also highlighted the importance of mechanical anchorages in limiting premature debonding. Ghobarah and Said (2001), El-Amoury and Ghobarah (2002), Mukherjee and Joshi (2005) developed effective selective rehabilitation schemes for RC beam column joints using advanced composite materials. Al-Salloum and Almusallam (2007), and Almusallam and Al-Salloum (2007) studied experimentally and analytically effectiveness of externally bonded CFRP sheets in improving shear strength and ductility of RC beam-column joints under simulated seismic forces. Ghobarah and El-Amoury (2005) developed effective rehabilitation systems to upgrade the resistance to bond-slip of the bottom steel bars anchored in the joint zone and to upgrade the shear resistance of beam-column joints.

A detailed review of literature shows that systematic studies to determine the behavior of the repaired and/or strengthened members under cyclic loading are still limited. Moreover, the behavior of seismically excited FRP repaired beam-column joints is not well established at various stages of response e.g. with and without shear reinforcement, before and after yielding of reinforcements, crushing of concrete, fiber fracture or de-bonding. Most of the paper does not demonstrate the rotational behavior of the joints rather beam and column deflection only. The present paper is also an effort in the same direction. In this paper, the behavior of joint with and without adequate joint shear strength (transverse reinforcement) subjected to cyclic lateral load histories so as to provide the equivalent of severe earthquake damage is compared. The efficiency and effectiveness of Carbon fiber reinforced polymers (CFRP) in upgrading the shear strength and ductility of seismically deficient exterior beam-column joints have also been studied.

The outcome of the study will unveil the behavior of the strengthened RC exterior BC joints and compare the behavior with the joints which lack in shear reinforcement. The research will also facilitate in developing methods of determining strength of retrofitted joints and identify suitable procedures to retrofit interior BC joints by CFRPs.

1.3   Objectives of the Study

The objectives of this study are as follows:

a. To study the behavior of RC Exterior beam-column joint with and without adequate shear reinforcement under cyclic horizontal loading.

b. To study the behavior and ductility of Exterior beam-column joint retrofitted by Fiber Reinforced Polymers (FRP).

1.4   Methodology

To investigate the behavior of the RC exterior BC joints retrofitted by FRP fabrics, incremental cyclic loading were provided with constant axial load on to the test samples. Half scale models had been constructed before strengthening the joints. Following parameters had been considered to investigate the behavior of the joints:

a. Exterior joints having identical concrete strength.

b. Exterior joints having different shear reinforcement.

c. Exterior joints retrofitted by wrapping beams and columns with CFRP fabrics.

Total three models had been constructed for the study as follows:

a. Two control models designated as Model-C1 (having 2 nos. ties at the joint) and Model-C2 (without any tie at the joint).

b. One models strengthened by CFRP Fabrics designated as Model-F.

1.5   Scope of the Study

This study considered only the BC exterior joints. All the samples had similar dimensions and strength. The joints were strengthened by CFRP only and other FRPs were not considered. Different method of FRP wrapping was not considered. The samples were subjected to static incremental cyclic loading.

1.6   Organization of the Thesis

The thesis paper is organized into total six chapters. Apart from chapter one, the following chapters are organized as follows:

Chapter Two: This chapter highlights theories on the ductility of the structure, types of joints and forces acting on the exterior joints in seismic condition. Existing seismic codes on exterior joints and use of FRPs are also discussed here. Some of the previous

studies related to ductility, behavior of the joints and joints strengthened by FRPs are also discussed in this chapter.

Chapter Three: Various types of materials had been used for constructing the models and strengthening the joints. Properties of these materials are discussed in detail in this chapter.

Chapter Four: Preparation of the models and strengthening joints are discussed deliberately in Chapter Four. This study needed deliberate experimental preparation and set up which are also discussed in this chapter.

Chapter Five: Experimental results and analysis are presented in Chapter Five. Behavior of joints strengthened by different methods is summarized in this chapter.

Chapter Six: This chapter summarizes the research and lists out the conclusions based on the outcome of the experimental study and recommend scopes for future studies.

CHAPTER TWO
LITERATURE REVIEW

2.1 General

This chapter discusses the ductility of the structure, types of joints and the forces acting on exterior joint under seismic condition, shear resisting mechanism in an exterior joint. This chapter extracted the BNBC-1993 on seismic detailing of beam-column joint. In this chapter, pros and cons of various retrofitting strategy are also highlighted. FRPs draw attention of the designers as a retrofitting material due to its high strength and easy placement. Material properties of the FRPs are discussed here and the use, application and design of FRP materials are also extracted from ACI 440.2r-08. Many researchers worked on ductility of the structures with poor joint configurations, strengthening them by various types of FRPs and evaluated their behavior under seismic conditions. Outcome of some of the researches are also discussed in this chapter.

2.2 Ductility of the Structure

It is essential that an earthquake resistant structure should be capable of deforming in a ductile manner when subjected to lateral loads in several cycles in the inelastic range. The structures subjected to cyclic loading need to dissipate the energy stored in it. Dissipation of energy can be explained by a simple phenomenon exhibited by an oscillator with a single degree of freedom as shown in Fig. 2.1.

In the elastic response, the oscillator has the maximum response at *a*. The area *oab* represents the potential energy stored when maximum deflection occurs. The energy is converted into kinetic energy when the mass returns to zero position. Fig. 2.1 (b) shows the oscillator forming a plastic hinge at a much lower response *c* when the deflection response continues along *cd, d* being the maximum response. The potential energy at the maximum response is now represented by the area *ocde*. When the mass returns to zero position, the part of the potential energy converted to kinetic energy is represented by *fde*, while the other energy under the area *ocdf* is dissipated by the plastic hinge by being transferred into heat and other forms of irrecoverable energy. From this, it can be concluded that the response in elastic state of a structure differs significantly from the

response of the same structure in elasto-plastic state where potential energy converts to kinetic and other forms of irrecoverable energy.

(a) Elastic Response   (b) Elasto-Plastic Response
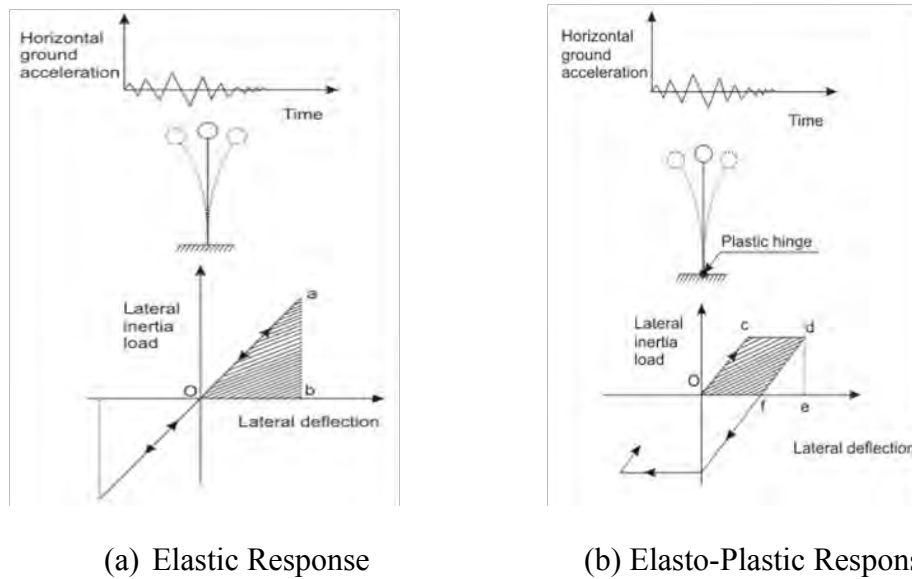
Fig. 2.1: Response of a Structure with Single Degree of Freedom (*www.nptel.ac.in*)

(a) Equal Maximum deflection   (b) Equal Maximum Potential Energy
Response   Response
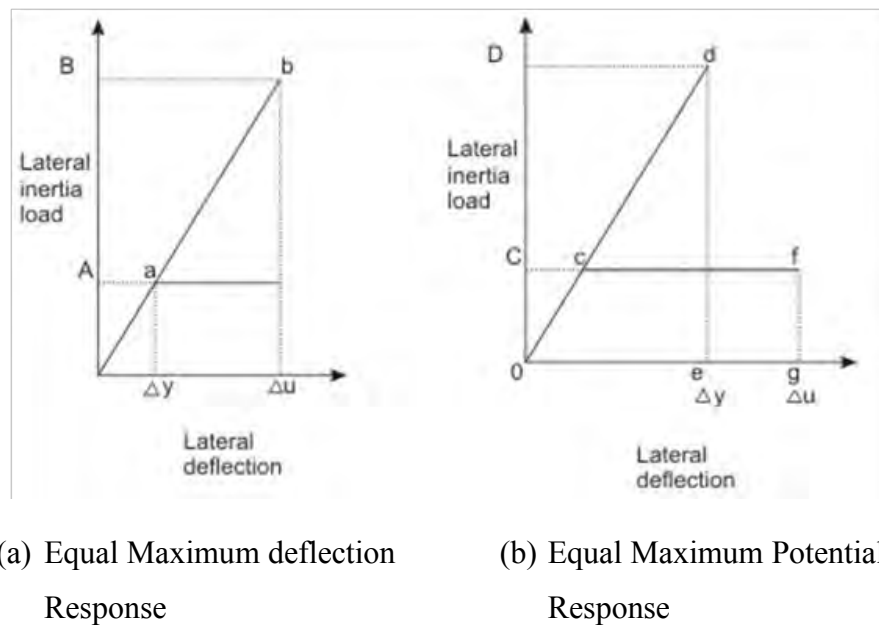
Fig. 2.2: Structural Response (*Paulay & Priestley, 1992*)

The displacement ductility factor μ, a measure of ductility of a structure, is defined as the ratio of Δ_u, and Δ_y, where Δ_u and Δ_y are the respective lateral deflections at the end of post elastic range and when the yield is first reached. Thus, we have μ (with respect to displacement) = Δ_u / Δ_y.

In a similar manner, the rotational ductility factor μ is defined as the ratio of θ_u and θ_y, where θ_u and θ_y are the respective rotations of at the end of post-elastic range and at the first yield point of tension steel. Thus, we have μ (with respect to rotation) = θ_u / θ_y.

2.3 Beam Column Joints

A beam-column joint is defined as the portion of a column within the depth of beams that frame into it (Nelson 1997). The functional requirement of a joint is to enable the adjoining members to develop and sustain their ultimate capacity. Earlier, the design of monolithic joints was limited to providing adequate anchorage (Nelson 1997). But now the design of the joints has got importance due to the consideration of large forces induced by the seismic events. The joints should have adequate strength and stiffness to resist the internal forces induced by the framing members.
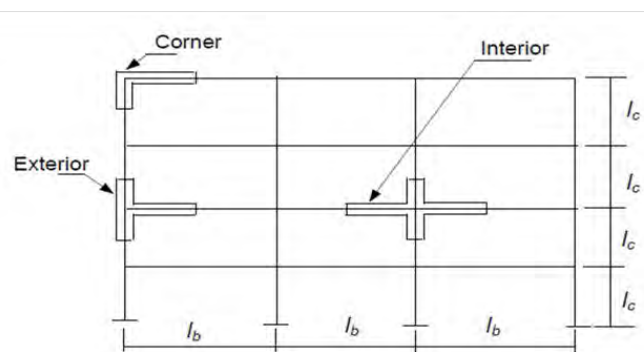
Fig. 2.3: Types of Joints (*Uma and Prasad 2006*)
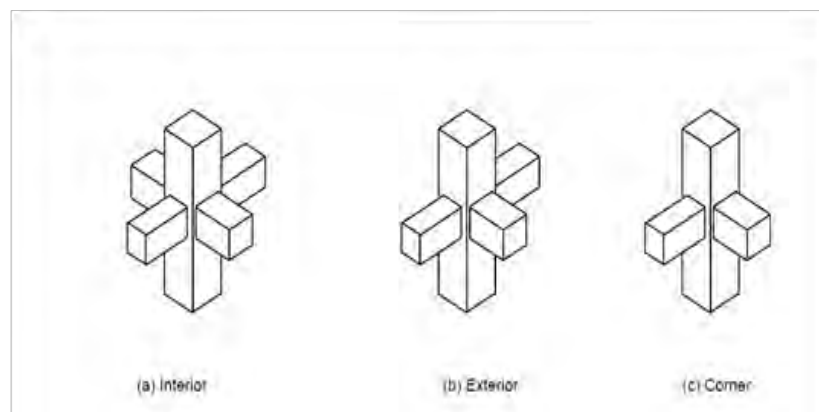
Fig. 2.4: Types of Joints (*Uma and Prasad 2006*)

2.3.1 Classification of Joints

The joints of a moment resisting RC frame can be classified as interior, exterior and corner joints as they are shown in Fig. 2.3 and 2.4. The joints must be able to resist the forces induced by the earthquake or cyclic loading. As this research deals with the behavior of external joints so the behavior of external joints under cyclic loading are discussed.

2.3.2 Behavior of Exterior Joint under Seismic Loading

In reinforced concrete members, the inelastic rotations spread over definite regions called as plastic hinges. During inelastic deformations, the actual material properties are beyond elastic range and hence damages in these regions are obvious. The plastic hinges are "expected" locations where the structural damage can be allowed to occur due to inelastic actions involving large deformations. Hence, in seismic design, the damages in the form of plastic hinges are accepted to be formed in beams rather than in columns. Mechanism with beam yielding is characteristic of strong-column-weak beam behavior in which the imposed inelastic rotational demands can be achieved reasonably well through proper detailing practice in beams. Therefore, in this mode of behavior, it is possible for the structure to attain the desired inelastic response and ductility. On the other hand, if plastic hinges are allowed to form in columns, the inelastic rotational demands imposed are very high that it is very difficult to be catered with any possible detailing. The mechanism with such a feature is called column yielding or storey mechanism.

BC joints have important roles to maintain the strength hierarchy of the moment resisting RC structure. The joints should have sufficient strength to resist the internal forces induced by the framing members. The failure should occur at the plastic hinges. The high internal forces developed at the plastic hinges cause critical bond conditions in the longitudinal reinforcing bars passing through the joint and also impose high shear demand in the joint core (Paulay et al. 1992., Hakuto et al. 2000). The joint behavior exhibits a complex interaction between bond and shear. The bond performance of the bars anchored in a joint affects the shear resisting mechanism to a significant extent.

The forces acting on an exterior joint can be idealized as shown in Fig. 2.5. The shear force in the joint gives rise to diagonal cracks thus requiring reinforcement of the joint. The detailing patterns of longitudinal reinforcements significantly affect joint

efficiency. Some of the detailing patterns for exterior joints are shown in Fig. 2.5(b) and Fig. 2.5(c). The bars bent away from the joint core (Fig. 2.5(b)) result in efficiencies of 25-40 % while those passing through and anchored in the joint core show 85-100% efficiency. However, the stirrups have to be provided to confine the concrete core within the joint.

(a) Forces   (b) Poor detail   (c) Satisfactory Detail
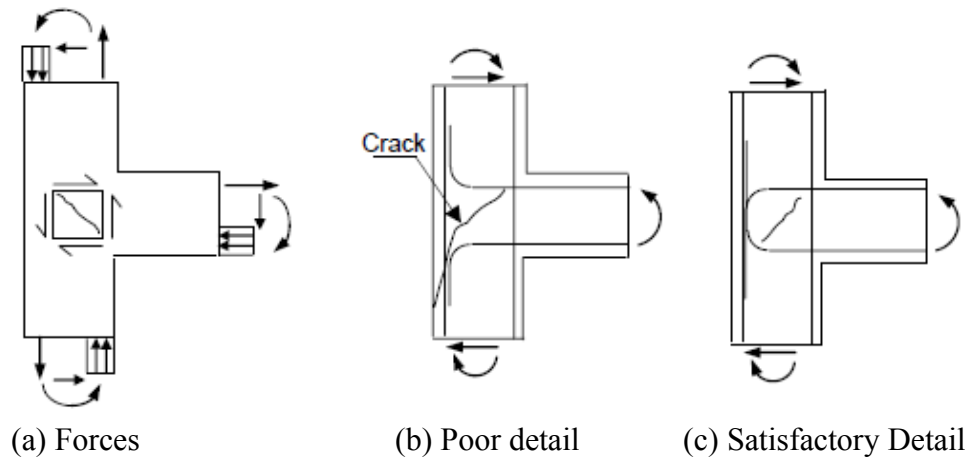
Fig. 2.5: Forces acting on Exterior Joint (Uma and Prasad 2005)

The moment resisting frame is expected to obtain ductility and energy dissipating capacity from flexural yield mechanism at the plastic hinges. Beam-column joint behavior is controlled by bond and shear failure mechanisms, which are weak sources for energy dissipation. The performance criteria for joints under seismic actions may be summarized as follows:

1. The joint should have sufficient strength to enable the maximum capacities to be mobilized in the adjoining flexural members.

2. The degradation of joints should be so limited such that the capacity of the column is not affected in carrying its design loads.

3. The joint deformation should not result in increased storey drift.

Bond requirement:

In exterior joints, the longitudinal reinforcement of beam that frames into the column terminates within the joint core. After a few cycles of inelastic loading, the bond deterioration initiated at the column face due to yield penetration and splitting cracks, progresses towards the joint core. Repeated loading will aggravate the situation and a complete loss of bond up to the beginning of the bent portion of the bar may take place. The longitudinal reinforcement bar, if terminating straight, will get pulled out due to

progressive loss of bond. The pull out failure of the longitudinal bars of the beam results in complete loss of flexural strength. This kind of failure is unacceptable at any stage. Hence, proper anchorage of the beam longitudinal reinforcement bars in the joint core is of utmost importance.

The pull out failure of bars in exterior joints can be prevented by the provision of hooks or by some positive anchorage. Hooks, as shown in Fig. 2.6 are helpful in providing adequate anchorage when furnished with sufficient horizontal development length and a tail extension. Because of the likelihood of yield penetration into the joint core, the development length is to be considered effective from the critical section beyond the zone of yield penetration. Thus, the size of the member should accommodate the development length considering the possibility of yield penetration.

When the reinforcement is subjected to compression, the tail end of hooks is not generally helpful to cater to the requirements of development length in compression. However, the horizontal ties in the form of transverse reinforcement in the joint provide effective restraints against the hook when the beam bar is in compression.
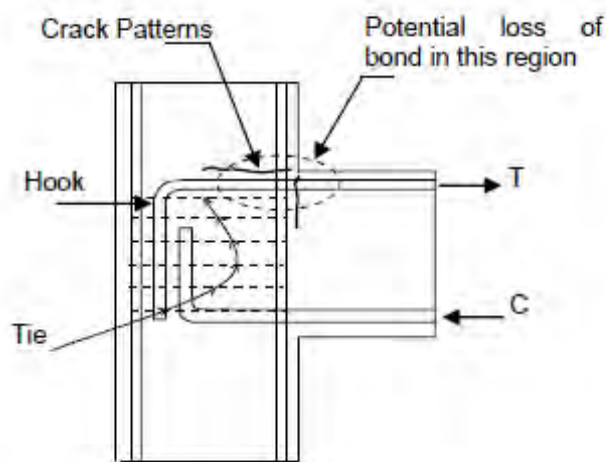
Fig. 2.6: Bond Stresses in a Exterior Joint (*Uma and Prasad 2006*)

The bond performance of the reinforcing bars is influenced by confinement, clear distance between bars and nature of surface between bars. The confinement in the joint region is obtained by the column axial load and horizontal reinforcement arresting the splitting crack (Ichinose 1991). Better bond performance is achieved when the clear distance between the longitudinal bars is less than 5 times the diameter of the bar

(Eligehausen et al. 1983). The deformed bar and concrete with high strength give better bond strength (Ichinose 1991).

Shear Requirement

The external forces induced by the earthquake or seismic loading acts on the face of the joints and develop large shear stresses within the joint. The combined effect of the shear stresses causes diagonal cracking when the tensile stresses exceed the tensile strength of the concrete. Extensive cracking occur due to load reversals under seismic events. Joints strength and stiffness are affected by extensive cracking causing joints to become flexible enough to undergo large deformation.

The centre to centre column distance and beam span is l_c and l_b, respectively. The forces and moment acing on the sub-assemblage, shear force and moment distribution of the exterior joints are shown in Fig. 2.7 (a), (b) and (c), respectively. The nature of the moment changes within the joint region. A steep gradient of the moment causes large shear force within the joint compared to the adjacent columns. The horizontal shear force within the joint region can be computed by equilibrium criteria.

Figure 2.7 shows the features of an exterior beam column joint where one beam frames into the column. Based on equilibrium principles, the column shear V_{col} and the horizontal shear force in the joint can be calculated as follows.

The column shear force is

$$V_{col} = \frac{T_b Z_b + V_b \frac{h_c}{2}}{l_c} \quad \text{...(2.1)}$$

Where l_c is the height of the storey and h_c is the depth of the column and Z_b is the lever arm of the tensile and compressive force. The horizontal shear within the joint core can be computed as

$$V_{jh} = V_{col}\left(\frac{l_c}{Z_b} - 1\right) - V_b\left(\frac{h_c}{2Z_b}\right) \quad \text{..(2.2)}$$

The horizontal shear force V_{jh} can be reduced by increasing the column depth h_c or increasing the vertical shear from beam V_b. Equations 2.1 and 2.2 can be simplified by considering the moment M_s and M_h and compressive and tensile strength of the reinforcing bars.

Column Shear, $V_{col} = \dfrac{M_h}{l_c}$ …………………………………………………………….(2.3)

And horizontal shear force

$V_{jh} = T - V_{col}$ ....(2.4)

(a) Forces on the column   (b) Bending moment   (c) Shear force
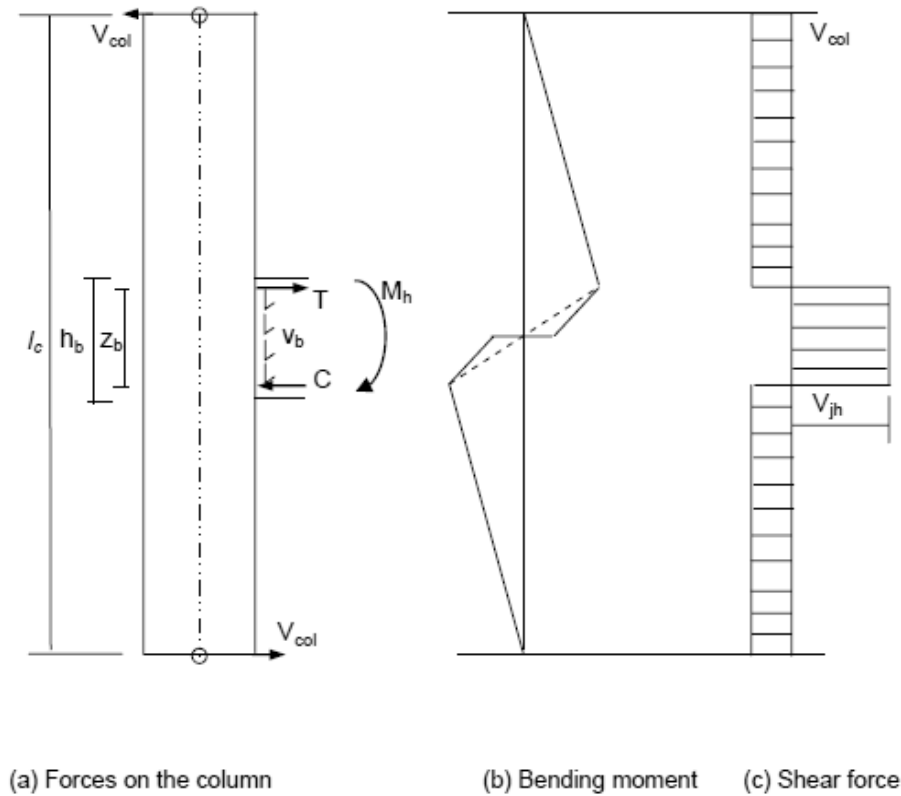
Fig. 2.7: Forces Acting on Exterior Joints (*Uma and Prasad 2006*)

The effective shear area is specified based on the dimension of the beam and column (Nelson 1997, Uma and Prasad 2004). The effective shear area of the joint A_j is defined by the width of the joint b_j and depth of the joint h_j. The area may not be as large as the column cross section since the width of the beam and column b_w and b_c respectively may differ from each other. When the beam width is less than the column width, the effective joint width is the average of the beam width and column width but should not exceed the beam width b_b plus one half the column depth h_c on each side of the beam (ACI 352.2r-02).

$b_j = \dfrac{b_b + b_c}{2}$ ....(2.5)

and must $be \leq (bb + hc)$ ....(2.6)

The beam width b_b is the average width of the beam framing into the column from opposite direction and h_j is taken as the depth of the column h_c.
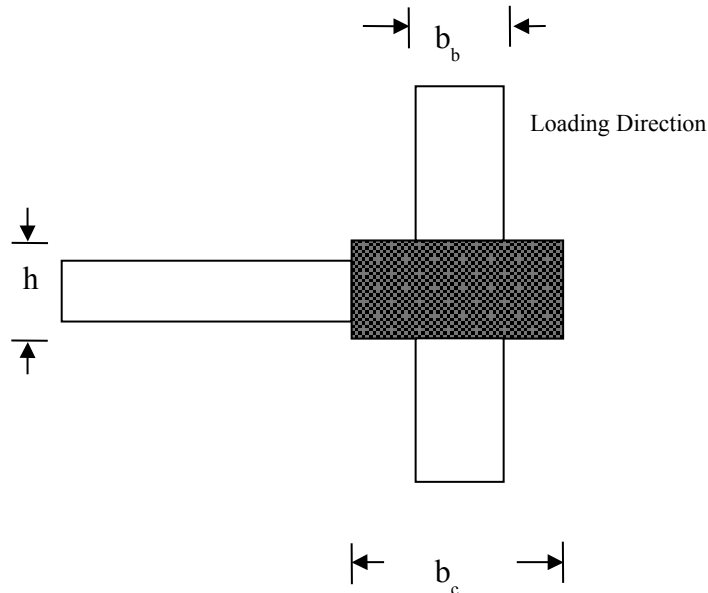
Fig. 2.8: Determination of Effective Joint Width (Nelson 1997)

The shear forces in the joint region develop diagonal compressive and tensile forces within the joint core. As a result, diagonal failure plane occurs within the joint region. The shear resisting mechanism is explained by strut and truss action (Fig. 2.9).

Diagonal concrete strut mechanism is formed by major diagonal compression force in the joint. This force is produced by the vertical and horizontal compression stresses and shear stresses on concrete at the beam and column critical section. The truss mechanism is a combination of bond stress transfer along the beam and column longitudinal reinforcement, the tensile resistance of lateral reinforcement and compressive resistance of uniform diagonal concrete struts in the panel region (Uma and Prasad 2006, Inchinose 1991).

The strength of the strut and truss mechanism depends on compressive strength of the concrete and tensile yield strength of the lateral reinforcement crossing the failure plane respectively. The strut mechanism can exist without any bond stress transfer along the beam column reinforcement within the joint where as truss mechanism can develop only when a good transfer is maintained along the beam and column reinforcement. With the outset of bond deterioration under seismic loading condition, the truss

mechanism starts to diminish and the diagonal strut mechanism must resist the most dominant part of the joint shear. The tensile force in the beam reinforcement not transmitted to the joint concrete by bond must be resisted by the concrete at the compression face of the joint thereby increasing the compression stress in the main strut. The strut is progressively weakened by the reversed cyclic loading. Concurrently, concrete compressive strength is reduced by the increasing tensile strain perpendicular to the direction of the main strut. The combination of these two phenomenon results in the failure of the concrete strut in shear compression. The principal role of the lateral reinforcement in this case is to confine the cracked core concrete (Uma and Prasad 2004). The shear force in the joint region is considered to be resisted by strut and truss mechanism.
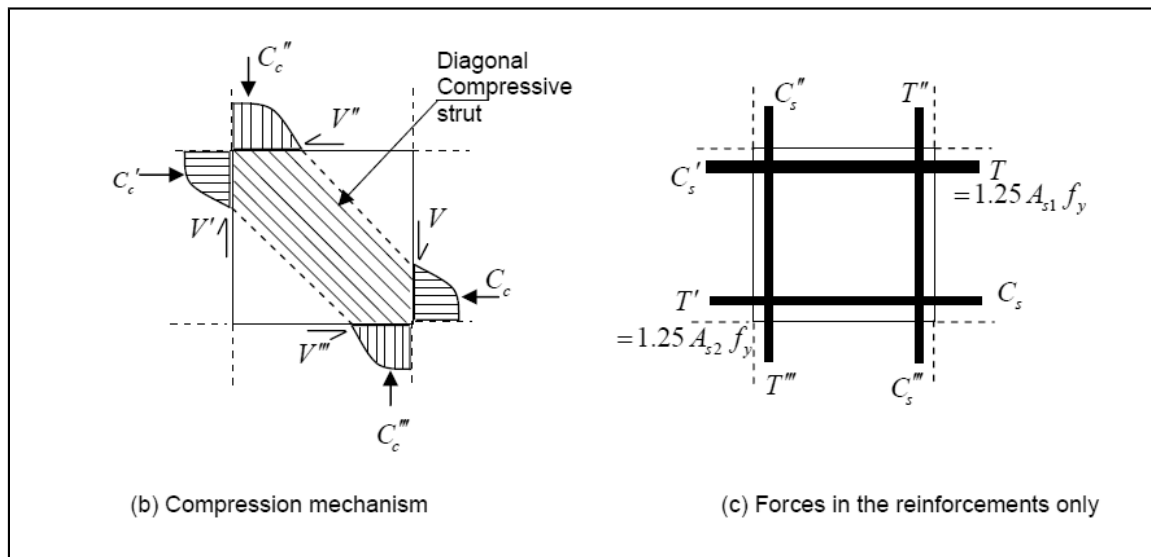
Fig. 2.9: Idealized Behavior of Beam Column Joint (*Uma and Prasad 2006*)

$$\mathbf{Vjh = Vch + Vsh} \quad\text{..(2.7)}$$

$$V_{jh}= (T-T_f)+C_f+C'_c+C'_s-V_{col} \quad\text{...(2.8)}$$

The shear strength provided by the truss mechanism can be written as

$$V_{sh}= V_{jh}-V_{ch} \quad\text{...(2.9)}$$

$$= Tb + C's - B's \quad\text{..(2.10)}$$

B'_s is the combined effect of compression and tension forces from the top reinforcement anchored in the joint core.

$$Tb = (T-Tf) = 1.25fy\,(As1-Asf) = 1.25fyAs \quad\text{...(2.11)}$$

$$C's = \gamma\, f_y\, A_s \quad \dots\dots\dots\dots\dots\dots\dots\dots\dots\dots\dots\dots\dots\dots\dots\dots\dots\dots\dots\dots\dots\dots(2.12)$$

is compression force developed in top beam bars. γ is the factor used to express the stress level in the bars in terms of yield stress.

After some bond deterioration, the compressive stress in the top beam reinforcement is not likely to exceed the stress level of $0.7 f_y$ (Cheung et al. 1991). At the same time, this stress cannot exceed $1.25\beta\, f_y$, here β is the ratio of bottom reinforcement to top reinforcement in the rectangular beam and is expressed as A_{s2}/A_s with $1.25\beta \geq \gamma \leq 0.70$. The value of γ may be less than 0.70 when the bottom reinforcement is about 50% of the top reinforcement or when the bottom beam reinforcement cannot yield at column face. Then $C's$ can be obtained from the actual stress, f_{s2} in the bottom reinforcement.

Shear reinforcement design is governed by minimum reinforcement area needed to support the truss mechanism and the maximum permissible area based on the limit stress corresponding to diagonal compression failure. Horizontal hoop reinforcement has to be designed for 40% of the total horizontal shear force as a minimum requirement (NZS 3101:1995). ACI353R-02 recommends horizontal reinforcement basing on the confinement of the core concrete required to maintain the axial load carrying capacity of the columns.

2.4 Requirement of Transverse Reinforcement for Joint

According to BNBC 1993, hoop reinforcement will be provided within the joint unless it is confined by the structural member. The requirement of transverse reinforcement of the column is determined by the following equations:

a. The volumetric ratio of spiral or circular hoop reinforcement, ρ_s shall be indicated by the following equation :

$$\rho_s = \frac{0.12 f'_c}{f_{yh}} \quad \dots\dots\dots\dots\dots\dots\dots\dots\dots\dots\dots\dots\dots\dots\dots\dots\dots\dots \quad (2.13)$$

And shall not be less

$$\rho_s = 0.45 \left[\frac{A_g}{A_c} - 1 \right] f'_c / f_y$$

$$\dots\dots\dots\dots\dots\dots\dots\dots\dots\dots\dots\dots\dots\dots\dots\dots\dots(2.14)$$

b. The total cross-sectional area of rectangular hoop reinforcement shall not be less than that given by the following equations :

$$A_{sh} = 0.3\left(sh_c f_c'/f_{yh}\right)\left[\left(A_g/A_{ch}\right)-1\right] \quad \text{.. (2.15)}$$

$$A_{sh} = \frac{0.09sh_c f_c'}{f_{yh}} \quad \text{...(2.16)}$$

c. Transverse reinforcement shall be provided by either single or overlapping hoops or cross ties of the same bar size and spacing. Each end of the cross ties shall engage a peripheral longitudinal reinforcing bars. Consecutive cross ties shall be alternated end for end along the longitudinal reinforcement.

d. If the design strength of member core satisfies the requirements of the specified loading combinations including earthquake effect, Equation 2.13 to 2.16 need not be satisfied.

Within the depth of the shallowest framing member, transverse reinforcement equal to at least one-half the amount mentioned above shall be provided where members frame into all four sides of the joint and where each member width is at least three-fourths the column width. At these locations, the spacing of the transverse reinforcement may be increased to 150 mm. Transverse reinforcement shall be provided through the joint to provide confinement for longitudinal beam reinforcement outside the column core if such confinement is not provided by a beam framing into the joint.

The nominal shear strength for the joint shall be taken not greater than the forces:

$1.66\sqrt{f_c'}A_j$ for joints confined on all four faces

$1.24\sqrt{f_c'}A_j$ for joints confined on three faces or on two opposite faces

$1.0\sqrt{f_c'}A_j$ for others

$$A_{sh} \geq \begin{cases} 0.5 \times \{0.3 s h_c \, [(A_g/A_{ch})- 1] \, (f'_c / f_{yh})\} \\ 0.5 \times [0.09 s h_c \, f'_c \, / f_{yh}] \end{cases}$$

$s \leq 150mm$

Transverse beams not shown for clarity

Elevation

$\geq 3c_2 / 4c_1$

$\geq 3c_1 / 4$

c_1

Plan
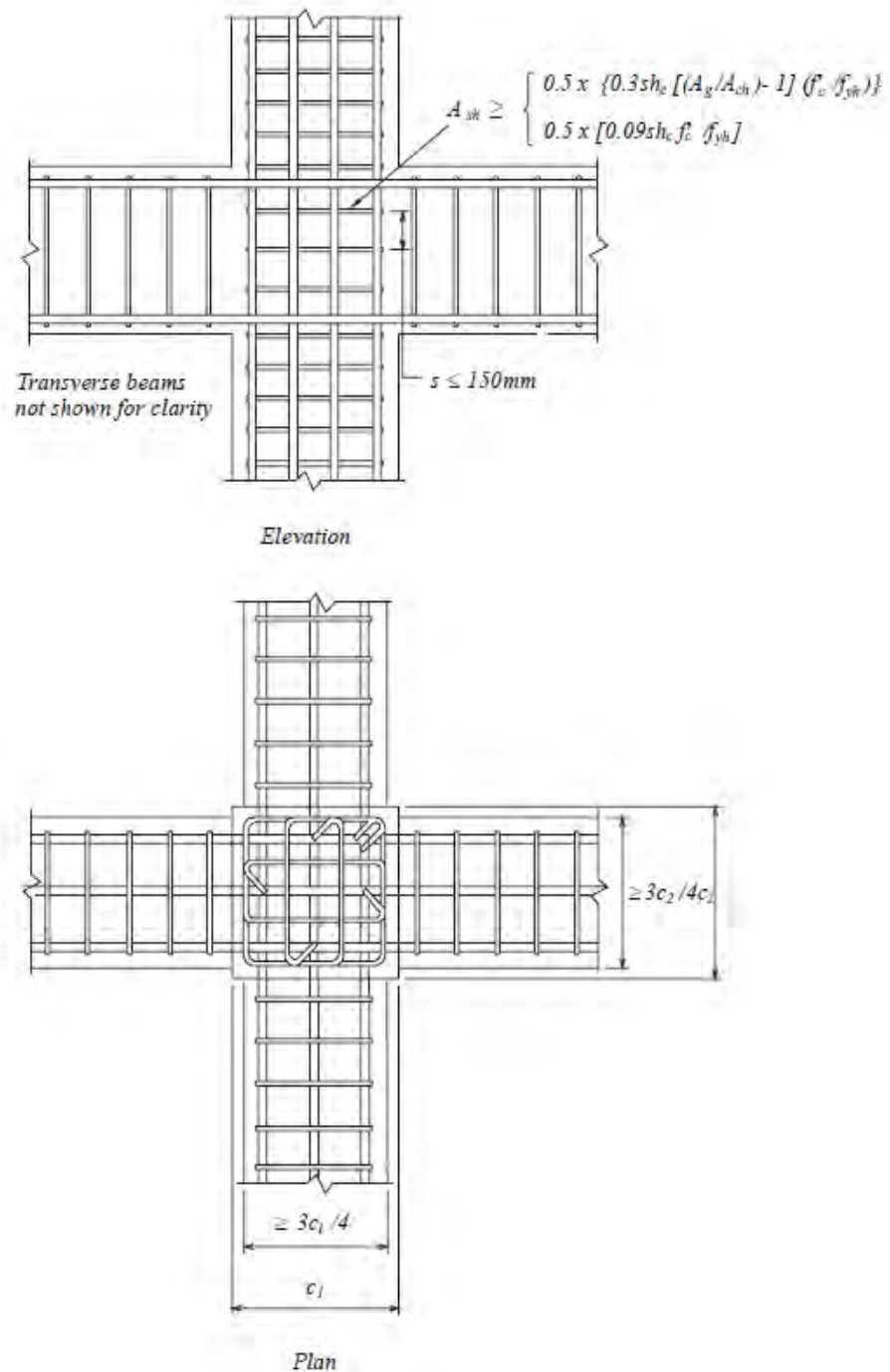
Fig. 2.10: Transverse Reinforcement Required for Joint Confined by Structural Member (BNBC 1993)

A member that frames into a face is considered to provide confinement to the joint if at least three-quarters of the face of the joint is covered by the framing member. A joint is considered to be confined if such confining members frame into all faces of the joint.

2.5   Retrofitting Strategy

Strengthening the existing structural members need numbers of consideration which were discussed in Chapter One. Joints can be retrofitted by increasing the dimensions or confinement. Usually, it is done by addition of longitudinal and shear reinforcement around the existing column and then casting with fresh concrete. Adequate measures are taken to ensure proper bond between the old and new concrete. Tsonos 2000 tested seven exterior reinforced concrete sub-assemblages that were subjected to severe earthquake damage. The specimens were repaired and strengthened by concrete jacketing and the strengthened specimens were tested again. He found that the repaired and strengthened specimens exhibited higher strength, higher stiffness and better energy dissipation capacity than the original specimens. Dhakal et al. 2003 tested a full scale interior beam-column joint that was first subjected to cyclic loading history to induce damage (Fig. 2.11(a)) and was then strengthened using RC jacket (Fig. 2.11 (b)) and then tested once again (Fig. 2.11 (c)). A much improved seismic response was obtained for the strengthened specimen. Shannag et al. 2002 tested five 1/3-scale interior beam column joints having old detailing, under cyclic lateral loading. The specimens were then repaired using high performance fiber reinforced concrete (HPFRC) jacket, all around the joint column regions, and tested again up to failure. Higher load levels, more ductile behavior, substantial energy dissipation and slower stiffness degradation were observed. Failure modes were modified from brittle shear in the joint to ductile beam failure through plastic hinge formation. Concrete jacketing is labor intensive and the building may be non-operational for long period. Relocation of existing occupancy also needs serious consideration. Increasing the existing dimensions may not be also possible due to various considerations like overhead clearance, existing facility dimension etc. FRPs are good alternatives to overcome these limitations. They can be placed easily without any significant increase in dimension and rehabilitation of existing occupancy is not required. But FRPs also have limitations as fire rating of FRP is poor, environmental exposures and the quality of substrate play significant roles in bond critical application. Many researchers have studied the behavior of FRP retrofitted structures and found that seismic as well as load bearing performance can be significantly increased by FRPs.

(a) Original Joint   (b) RC Jacketing   (c) Strengthened Joint
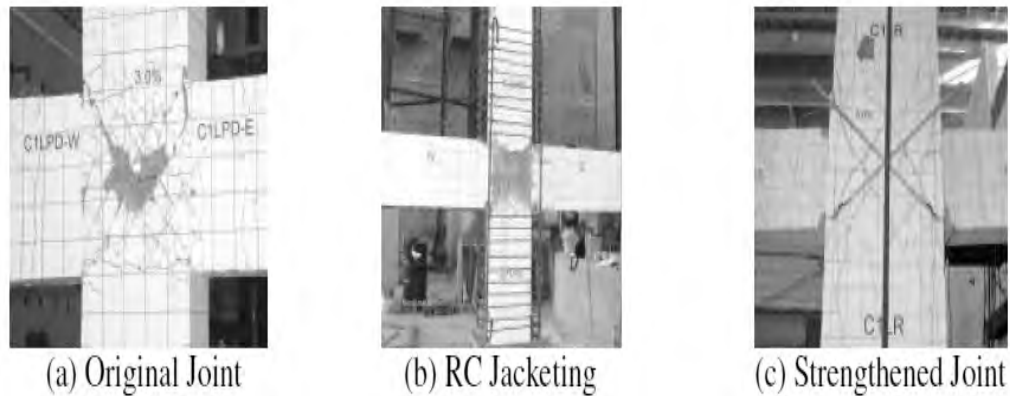
Fig. 2.11: Retrofitting Damaged Interior Joint (Dakhal et al. 2003)

2.6   Guidelines for Use and Design of FRP Systems

2.6.1   Use of FRP system

The guide for the design and construction, use and applicability for externally bonded FRP system for strengthening concrete structure is given in detail in ACI 440.2r-08.

ACI recommends FRP system to be used as additional tensile reinforcement and not as compressive reinforcement. ACI recommends a total evaluation of the structure before strengthening by FRPs. The overall evaluation should include a thorough field inspection, a review of existing design or as-built documents, and a structural analysis in accordance with ACI 364.1R. Existing construction documents for the structure should be reviewed, including the design drawings, project specifications, as-built information, field test reports, past repair documentation, and maintenance history documentation. The engineer should conduct a thorough field investigation of the existing structure in accordance with ACI 437R or other applicable documents. The tensile strength of the concrete on surfaces where the FRP system may be installed should be evaluated by conducting a pull-off adhesion test in accordance with ACI 503R.

FRP-strengthened structures should comply with all applicable building and fire codes. Smoke and flame spread ratings should be determined in accordance with ASTM E 84. Coatings can be used to limit smoke and flame spread. Due to the low temperature resistance of most FRP materials, the strength of externally bonded FRP systems is assumed to be lost completely in a fire. For this reason, the structural member without

the FRP system should possess sufficient strength to resist all applicable loads during a fire. The physical and mechanical properties of the resin components of FRP systems are influenced by temperature and degrade above their glass transition temperature T_g. The T_g is the midpoint of the temperature range over which the resin changes from a hard brittle state to a softer plastic state. This change in state will degrade the properties of the cured laminates. The T_g is unique to each FRP system and ranges from 60º to 82º C (140º to 180º F) for existing, commercially available FRP systems. The maximum service temperature of an FRP system should not exceed the T_g of the FRP system. The T_g for a particular FRP system can be obtained from the system manufacturer.

Concrete distress, deterioration and corrosion of existing reinforcing steel should be evaluated and addressed before the application of the FRP system. Concrete deterioration concerns include but are not limited to, alkali-silica reactions, delayed ettringite formation, carbonation, longitudinal cracking around corroded reinforcing steel and laminar cracking at the location of the steel reinforcement. The condition and strength of the substrate should be evaluated to determine its capacity for strengthening of the member with externally bonded FRP reinforcement. The bond between repair materials and original concrete should satisfy the recommendations of ACI 503R or Section 3.1 of ICRI Guideline No. 03733.

The tensile strength of concrete should be at least 1.4 MPa (200 psi) as determined by using a pull-off type adhesion test as in ACI 503R or ASTM D 4541. FRP systems should not be used when the concrete substrate has a compressive strength (fc') less than 17MPa (2500 psi). Contact-critical applications, such as column wrapping for confinement that rely only on intimate contact between the FRP system and the concrete, are not governed by this minimum value. Design stresses in the FRP system are developed by deformation or dilation of the concrete section in contact-critical applications. The application of FRP systems will not stop the ongoing corrosion of existing reinforcing steel. If steel corrosion is evident or is degrading the concrete substrate, placement of FRP reinforcement is not recommended without arresting the ongoing corrosion and repairing any degradation to the substrate. The mechanical properties (for example, tensile strength, strain, and elastic modulus) of some FRP systems degrade under exposure to certain environments, such as alkalinity, salt water, chemicals, ultraviolet light, high temperatures, high humidity, freezing and thawing

cycles. The material properties used in design should account for this degradation as given in Table 2.1.

Table 2.1: Environmental Reduction Factor for Various FRP Systems and Exposure Conditions (ACI 440.2r-08)

Exposure Condition	Fiber Type	Environmental Reduction Factor, C_E
Interior Exposure	Carbon/epoxy	0.95
	Glass/epoxy	0.75
	Aramid/epoxy	0.85
Exterior Exposure	Carbon/epoxy	0.85
	Glass/epoxy	0.65
	Aramid/epoxy	0.75
Aggressive Environment (Chemical Plants/Waste Water Treatment Plants)	Carbon/epoxy	0.85
	Glass/epoxy	0.50
	Aramid/epoxy	0.70

The shear strength of existing concrete beams and columns can be increased by FRP system by wrapping or partially wrapping the members. Orienting the fibers transverse to the axis of the member or perpendicular to potential shear cracks is effective in providing additional shear strength. Increasing the shear strength can also result in flexural failures, which are relatively more ductile in nature as compared to shear failures.

The three types of FRP wrapping schemes used to increase the shear strength of prismatic, rectangular beams, or columns are illustrated in Fig. 2.12. Completely wrapping the FRP system around the section on all four sides is the most efficient wrapping scheme and is most commonly used in column applications where access to all four sides of the column is usually available. In beam applications, where an integral slab makes it impractical to completely wrap the member, the shear strength can be

improved by wrapping the FRP system around three sides of the member (U-wrap) or bonding to the two sides of the member.
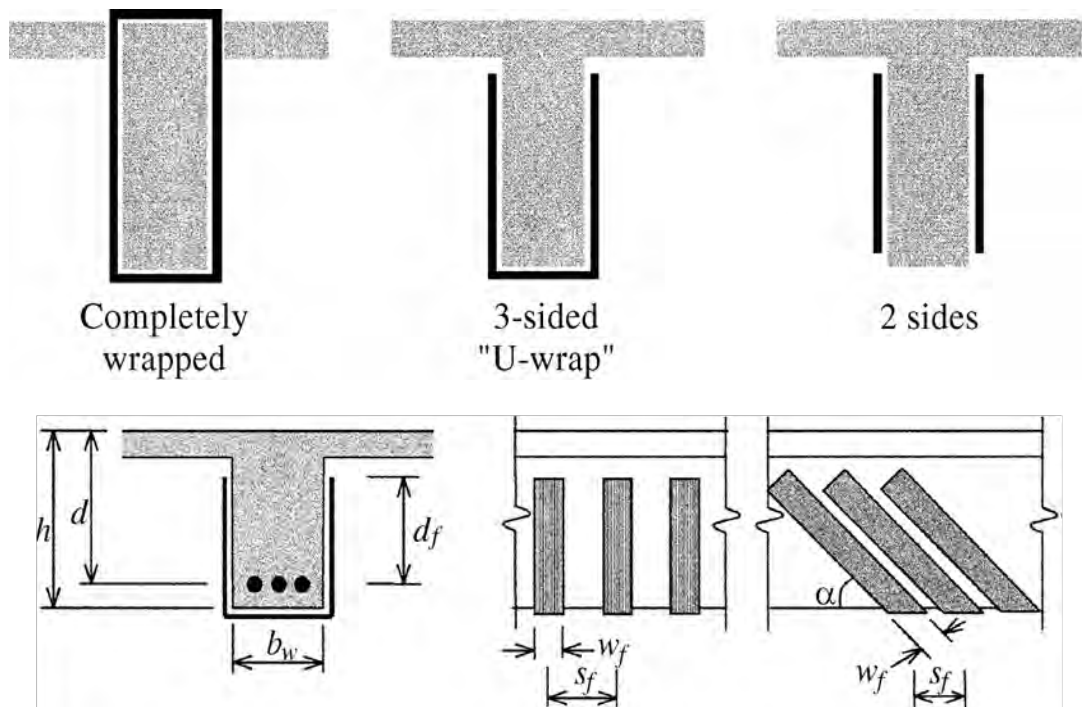
Fig. 2.12: Shear Strengthening of RC Beam by FRP Fabrics (ACI 440.2r-08)

Mechanical anchorages can be used at termination points to develop larger tensile forces (Khalifa et al. 1999). The effectiveness of such mechanical anchorages, along with the level of tensile stress they can develop, should be substantiated through representative physical testing. In no case, however, should the effective strain in FRP laminates exceed 0.004.

2.6.2 Design of FRP System for shear strengthening

The nominal strength of a concrete member strengthened with a FRP system should exceed the required shear strength. The required shear strength on an FRP strengthened concrete member should be computed with the load factors required by ACI 318-99. The shear strength should be calculated using the strength reduction factor Φ required by ACI 318-99. The nominal shear strength of the FRP-strengthened concrete member can be determined by adding the contribution from the reinforcing steel (stirrups, ties, spiral) and the concrete. An additional reduction factor Ψ_f is applied to the contribution of the FRP system.

$$\Phi Vn \geq Vu \qquad \text{...(2.17)}$$

$$\Phi Vn = \Phi(Vc + Vs + \Psi f\, Vf\,) \qquad \text{... (2.18)}$$

For bond-critical shear reinforcement, an additional reduction factor 0.85 and for contact-critical shear reinforcement, additional shear reinforcement 0.95 is recommended.

The contribution of the FRP system to shear strength of a member depends on the fiber orientation and assumed crack pattern (khalifa et al. 1998). The shear strength provided by the FRP reinforcement can be determined by calculating the force resulting from the tensile stress in the FRP across the assumed crack. The shear contribution of the FRP shear reinforcement is given by equation

$$Vf = \frac{A_{fv}\, f_{fe}\, (\sin[\alpha + \cos\alpha)\, d_f]}{S_f} \qquad \text{...(2.19)}$$

Where $A_f = 2nt_f W_f$ ....(2.20)

The tensile stress in the FRP shear reinforcement at ultimate is directly proportional to the level of strain that can be developed in the FRP shear reinforcement at ultimate.

$$f_{fe} = \varepsilon_{fe}\, E_f \qquad \text{...(2.21)}$$

The effective strain is the maximum strain that can be achieved in the FRP system at the ultimate load stage and is governed by the failure mode of the FRP system and of the strengthened reinforced concrete member. For reinforced concrete column and beam members completely wrapped by the FRP system, loss of aggregate interlock has been observed to occur at the fiber strains less than the ultimate fiber strain. For this, the maximum strain used for design should be limited to 0.4% for the application that can be completely wrapped with FRP system.

$$\varepsilon_f = 0.004 \leq 0.75\varepsilon_f$$

FRP systems that do not enclose the entire cross section (two or three sided wrapping) have been observed delaminate from the concrete before the loss of aggregate interlock of the section. For this reason, bond stress should be analyzed to determine the usefulness of these systems and the effective strain level that can be achieved. The effective strain is calculated using bond reduction coefficient k_v applicable to shear.

The bond reduction coefficient is a function of the concrete strength, the type of wrapping scheme used and the stiffness of the laminate. The bond reduction coefficient can be computed from equation 2.22 to 2.25 (khalifa et al. 1990)

$$k_v = \frac{k1\ k2\ Le}{468\ \mathcal{E}fu} \leq 0.75 \qquad \text{U. S Unit} \dots\dots\dots\dots\dots\dots\dots\dots\dots\dots\dots\dots\dots\dots\dots\dots\dots\dots 2.22$$

$$k_v = \frac{k1k2Le}{11900\ \mathcal{E}fu} \leq 0.75 \qquad \text{S.I Unit} \dots\dots\dots\dots\dots\dots\dots\dots\dots\dots\dots\dots\dots\dots\dots\dots 2.23$$

The active bond length L_e over which the majority of the bond stresses is maintained. The length is given by the equation

$$Le = \frac{2500}{(nt_fE_f)^{0.58}} \qquad \text{U. S. Unit} \dots\dots\dots\dots\dots\dots\dots\dots\dots\dots\dots\dots\dots\dots\dots\dots 2.24$$

$$Le = \frac{23,300}{(nt_fEf)^{0.58}} \qquad \text{S.I. Unit} \dots\dots\dots\dots\dots\dots\dots\dots\dots\dots\dots\dots\dots\dots\dots\dots 2.25$$

The bond reduction coefficient also relies on two modification factors k_1 and k_2, that account for the concrete strength and FRP wrapping scheme used respectively.

$$k1 = \left(\frac{fc'}{4000}\right)^{2/3} \qquad \text{U.S. Unit} \dots\dots\dots\dots\dots\dots\dots\dots\dots\dots\dots\dots\dots\dots\dots\dots 2.26$$

$$k1 = \left(\frac{fc'}{27}\right)^{2/3} \qquad \text{S.I. Unit} \dots\dots\dots\dots\dots\dots\dots\dots\dots\dots\dots\dots\dots\dots\dots\dots 2.27$$
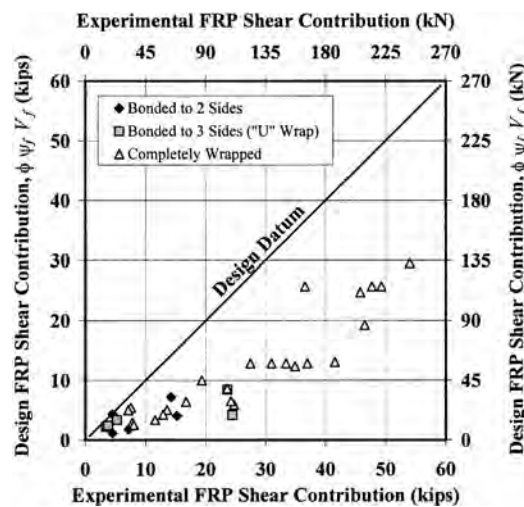
Fig. 2.13: Comparison of the Experimental Results to the Results using the Design Procedure (ACI 440.2r-02)

The methodology for determining k_v has been validated for members in regions of high shear and low moment, such monotonically loaded simply supported beams. Although the methodology has not been confirmed for shear strengthening is areas subjected to combined high flexural and shear stresses or in regions where the web is primarily in compression, k_v is suggested to be sufficiently conservative for such cases.

Spaced FRP strips used for shear strengthening should be investigated to evaluate their contribution to the shear strength. Spacing should adhere to the limits set by ACI 318-99 for internal steel shear reinforcement. The total shear reinforcement should be taken as the sum of the contribution of FRP and steel shear reinforcement. The total shear reinforcement should be limited on the criteria given in the following equations:

$$V_s + V_f \leq 8\sqrt{f_c'}\, b_w d$$ ....(2.28)

$$V_s + V_f \leq 0.66\sqrt{f_c'}\, b_w d$$ ....(2.29)

2.6.3 Detailing of FRP system

Detailing of FRP system for strengthening the concrete structure typically depends on the geometry of the structure, the soundness and quality of the substrate, and the levels of load that are to be sustained by the FRP sheets or laminates. Many bond-related failures can be avoided by following these general guidelines for detailing FRP sheets or laminates:

a. Do not turn inside corners;

b. Provide a minimum 13 mm (1/2 in.) radius when the sheet is wrapped around outside corners; and

c. Provide sufficient overlap when splicing FRP plies.

2.7 Literature Review on Earlier Research

2.7.1 Pantelidies et al. (2000)

The experiment was conducted on exterior beam column joints to compare the behavior of the FRP retrofitted joints to the as built joints which lack in adequate shear reinforcement. The as built joint achieved 66% of the shear strength allowed by the ACI 352R Code [1991] for exterior Type 2 joints. The FRP composite wrap can increase the strength, ductility, and drift performance of the joint. The FRP composite alleviates splitting cracks around the outer column bars such that the concrete cover does not spall off. The FRP composite also provided containment and partial

confinement of the joint's core concrete. The as built specimens maintained 90% of the axial load in the column at a drift level of 2.3%, whereas the FRP retrofitted specimens maintained 80% of the axial load at a drift level of 4.6%. The joint shear strength of the FRP retrofitted joint was 45% higher than that of the as-built joint.

2.7.2 Pampanin et al. (2002)

Pampanin et al. 2002 carried out an experiment on six different types of exterior and interior joints designed for gravity loads only. Plane reinforcement was used in the test models. Structural inadequacies, as typical of the Italian construction practice before the introduction of seismic code provisions in the mid- 70's were reproduced. The combined use of smooth reinforcing bars with end-hook anchorage as well as lack of any capacity design considerations showed to be a critical source of significantly brittle damage mechanisms as in the case of exterior joints, where additional sources of shear transfer mechanisms cannot develop after first diagonal cracking in the joint. An apparent satisfactory level of deformability as well as ductility, due to the combined effects of slippage phenomena and low column reinforcement ratio, were observed in knee and interior cruciform subassemblies, where no joint degradation occurred and column flexural damage dominated the behavior. Moreover, the comparison of different anchorage solutions for beam-bars in interior specimens showed a higher deformability due to slippage phenomena, without resulting in flexural strength reduction. When considering the overall seismic behavior of a frame structure, the implications of the aforementioned flexural damage on the overall seismic behavior might be significant, with soft storey mechanisms being likely to occur at early stages.

2.7.3 Mukharjee et al. (2002)

The experiment was carried out to investigate the behavior of RCC joint with and without adequate shear reinforcement in the joint region. The joints were strengthened by different types of FRPs in different configurations before and after failure and their behavior was compared with the control specimen. The specimens with adequate shear reinforcement and strengthened with FRPs exhibited higher dissipation of energy and ultimate deformation than controlled specimens. The main cause for the superior performance of the FRP strengthened is the confinement of concrete by FRP wraps. The damaged specimen were strengthened by FRP wraps and exhibited better performances in terms of ultimate load carrying capacity, displacement under ultimate load and energy dissipation energy. Non-ductile joints strengthened by FRP also

exhibited better performance and their performance depends on the number of layers of FRP wrapping. But the displacement at yield increased to a much lesser extent than the load.

2.7.4 Al-Salloum et al. (2007)

The study was carried out to see behavior of FRP strengthened joints with or without mechanical anchorage. Externally bonded FRP sheets can effectively improve the shear strength and ductility of beam column joints but the magnitude of effectiveness depends how the sheets were attached to joints and whether mechanical anchorage was used or not. The effect of two different schemes of rehabilitation was studied in upgrading the joint. In the first scheme, CFRP sheets were epoxy bonded to the joint, beams, and part of the column regions. In the second scheme, however, sheets were epoxy bonded to the joint region only but they were effectively prevented against any possible de-bonding through mechanical anchorages. It was observed that Scheme 1 is an efficient scheme because it upgrades both the joint and the beam. However, due to the absence of any mechanical anchorages in this scheme, at higher stages of loading de-bonding bulging of externally bonded CFRP sheets occurred, which allowed cracks to form and widen under the fiber sheets. Scheme 2 is an economical and effective scheme for joint strengthening, as in this scheme CFRP sheets were applied in such a way that the possibility of de-bonding is eliminated. Moreover, this scheme makes the joint so strong that failure is directed to the beams. The effectiveness of the two above-mentioned schemes of strengthening was also examined through shear distortion hysteretic curves and it was observed that externally bonded CFRP sheets make the joint stiffer against distortion. The results of the present study infer that, for field applications, it is very much necessary to decide judiciously and carefully which scheme is suitable for strengthening a deteriorated or deficient BC joint. This is because strengthening of a joint and its adjacent members with CFRP sheets at one place can substantially improve the shear strength and ductility of the joint but at the same time it may also shift the failure mode from the joint to the adjacent member e.g., beam or column or vice versa.

2.7.5 Shiohara (2008)

Shiohara 2008 reexamined twenty reinforced concrete interior beam-to-column joint failed in joint shear. The data indicated that joint shear stress had increased in the most specimens, even after apparent joint shear failure starts, while beam moment decreases

due to decrease of flexural resistance which is caused by reduction of distance between stress resultants in beam at column face. The cause of the deterioration of story shear is identified to be a degrading of moment resistance of joint, originated from a finite upper limit of anchorage capacity of beam reinforcements through the joint core. To reflect the fact, Hitoshi introduced a new mathematical model and proposed a new approach for the design of beam-to-column joint in seismic zone based on the prediction of the model.

2.7.6 Shiohara et al. (2010)

Shiohara et al. 2010 carried out the experiment on twenty interior beam column joints on a one third scale. They investigated the effects of design parameters of joints on lateral capacity and post yielding behavior. Three major parameters of the test program were (1) amount of longitudinal reinforcement, (2) column-to-beam flexural strength ratio, and (3) column-to-beam depth ratio. The test results indicate that maximum story shear of some specimens fall 5% to 30% short of the story shear calculated from the flexural strength of the beam or the column, although the joints have some margin of the nominal joint shear strength by 0% to 50% compared to the calculated values by a current seismic provision. The extent of insufficiency in the story shear was larger if the flexural strength of the column is equal or nearer to the flexural strength of the beam, and if the depth of the column is larger than that of the beam. This kind of design parameters are common to the existing reinforced concrete buildings and not addressed in many seismic design codes.

2.7.7 Ilki et al. (2011)

The main purpose of this study was to investigate the seismic behavior of FRP-retrofitted existing insufficient exterior beam-column joints built with plain bars and low-strength concrete. Although FRP-retrofitted specimens with welded hooks of beam longitudinal bars achieved the flexural capacity of the framing beam, the reference specimens and FRP-retrofitted specimen without welding of hooks of beam longitudinal bars could not reach the flexural capacities of the framing beam and columns. It was clearly seen that the FRP application only was not sufficient to prevent slippage of the beam longitudinal bars. When the joint is only rehabilitated with welding procedure, the strength was governed by the flexural capacity of the beam and the specimen could keep its strength until the drift ratio of 4% was reached. However, after 4% drift, the shear damage in the joint caused a sharp decrease in the strength of

the specimen. When joints are further retrofitted with FRP sheets after the rehabilitation of anchorage of beam longitudinal bars through welding, the strength decay was significantly retarded. Through adequate design and detailing of FRP retrofit, the specimens kept their strength until the drift ratios reached approximately 9 to 10%. Strain measurements on FRP sheets on joints showed that as the amount of the FRP sheets increased, the strains were lower. This indicates the formation of relatively less joint shear deformation and damage after FRP retrofitting. In all FRP-retrofitted specimens, FRP strains varied between 0.1% and 0.4% at peak load levels. After exceeding the lateral-load capacity of the specimens, FRP strains increased with increasing drift ratios, and strains on FRP sheets in diagonal directions reached approximately 1.5%. Consequently, it was concluded that effective FRP strain can be considered as 0.4% in the force-based design of FRP-retrofitted joints (approximately 25 to 30% of the ultimate FRP strain for this case). However, if a displacement-based design is carried out, FRP strains exceeding 0.4% can be considered, provided that the FRP retrofit design is sufficient to obtain ductile behavior. A simple procedure was used to calculate the contributions of concrete and FRP sheets to the shear capacity of the joint by utilizing truss analogy and Mohr's stress circle. The reduction of shear capacities of concrete and FRP was taken into account as a function of the achieved drift ratio, considering the damage of concrete and FRP in the joint. Predicted shear capacities matched well with experimental results of both reference and FRP-retrofitted specimens until large drifts were reached.

2.7.8   Li Bing et al. (2011)

The experiment was conducted on four full scale interior beam column joints without any shear reinforcement. The specimens had different column to beam width ratio. Under the application of cyclic loading, the control specimens exhibited flexural crack at 0.4% drift ratio and the cracking was severe during a drift ratio of 3%. The damaged control specimens were repaired using GFRP and CFRP wrapping to restore the strength. The repaired specimens were retested and their performances were compared with that of the control specimen. The result showed that the repair of damaged RC beam-wide column joints by FRP can restore the performance of the damaged joints.

2.7.9   Murshed and Ahmed (2011)

Murshed and Ahmed 2011 carried out seismic analysis on eight soft story structures which were retrofitted with FRP wraps. It was found that seismic performance of the

soft story structures can be improved by FRP wraps. Improve in the lateral strength was negligible due to wraps but ductility improvement was quite satisfactory. It was also found that hinge formation at the performance level had been significantly improved. No collapse prevention hinge was found in the retrofitted structure. At most of the times, the hinge for retrofitted structure remained within the immediate occupancy level and very few at life safety level which is very desirable scenario for structures in seismic prone areas.

2.7.10 Xiaobing et al. (2013)

The experiment was carried out to study the mechanical behavior of square FRP-strengthened concrete columns subjected to concentric and eccentric compression loading. Basing on the study, a numerical analysis model was developed and verified against the test results of square concentrically loaded plain concrete columns and square eccentrically loaded RC Columns. An analytical formula for the increase of maximum compression load for FRP strengthened columns with respect to non strengthened columns was developed and verified by the test results of the 23 square and rectangular RC columns. It was found that the increase of the maximum compression load of the strengthened concrete columns increase linearly with increased amount of FRP sheets used decreased linearly with increased load eccentricity and exponentially with increased concrete compression strength with respect to non-strengthened columns. This implies that FRP wrapping might be most suitable for low strength concrete members.

2.8 Summary of Literature Review

The external forces induced by the earthquake or seismic loading acts on the face of the joints and develop large shear stresses within the joint. The combined effect of the shear stresses causes diagonal cracking when the tensile stresses exceed the tensile strength of the concrete. Extensive cracking occur due to load reversals under seismic events and cause the joints to become flexible enough to undergo large deformation. The performance of the joint can be enhanced by increasing the bond strength between the reinforcing bars and concrete and increasing the confinement. Bond strength can be increased by increasing the depth of the column and confinement can be increased by providing horizontal reinforcement. Seismic detailing of new structures is given in detail in BNBC-1993. In case of existing structures with poor seismic detailing, seismic performances can be increased by concrete jacketing and increasing the column

dimension. But, retrofitting strategy depends on many other factors. FRPs are high strength materials but exhibit linear elastic properties. Their performance depends on many factors including environmental and exposure conditions, existing concrete surface and risk to fire hazards. Many researchers worked on strengthening the existing RC BC joints by FRPs of various types. Flexural and shear capacities of beam can be enhanced by FRP plates and fabrics. Axial capacity of columns can be enhanced by confinement with FRP fabrics. The joint capacity can be increased also by FRPs as they increase confinement and containment of the concrete.

CHAPTER THREE
MATERIAL PROPERTIES

3.1   General

This chapter discusses the properties of various materials used in this research work. Cement, sand, brick coarse aggregates and steel reinforcement had been used for the control and retrofitted specimen. CFRP fabrics had been used with epoxy primer and saturant for retrofitting the joints.

3.2   Sand

Sands are fine aggregates used in the cement concrete to fill the voids of coarse aggregates and they take 35% to 45% by mass or volume of total aggregates (Neville1995). Physical and chemical properties of the sand influence the strength and durability of concrete. Coarse Sylhet sand has been used for all specimens. Sylhet sand is natural sand produced by erosion of natural rocks. Important qualities of sand those influence the quality of fresh and hardened concrete are specific gravity, absorption capacity, moisture content, grading and chemical properties. If the dry sand absorbs large amount of water then w/c ratio of the fresh concrete will be changed and if the sand contains free water then the free water participates in the hydration process affecting the design strength of concrete. Gradation of fine aggregates has direct impact on workability of fresh concrete and strength of hardened concrete. Higher percentage of fines will add to workability of fresh concrete (Neville1995).

Absorption capacity of the sands was 4% but moisture content varies widely due to monsoon rain. Moisture content of the aggregates had been measured before every batch and water content of the fresh concrete was adjusted. FM of the sands had been found 2.57 by sieve analysis. Gradation of the sands is shown in Fig. 3.1. Detail data of the sieve analysis of sand is given in Table A.1 in Appendix A.
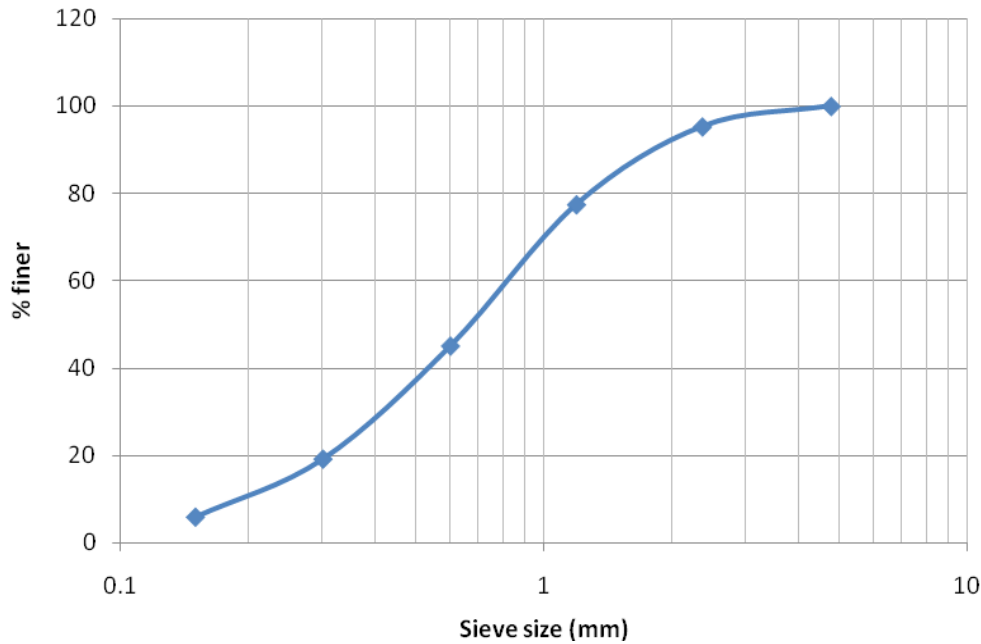
Fig. 3.1: Grain size distribution curve of Fine Aggregates

3.3   Coarse Aggregate

Strength and durability of concrete depend on the type, quality and size of the aggregates. In Bangladesh, stone particles and brick chips are mostly used as coarse aggregate. According to BNBC (1993) maximum size of the aggregates should not exceed 1/5th of the narrowest dimension between two sides, 1/3rd depth of the slab and 3/4th of the clear spacing between the reinforcing bars and the form works (BNBC 1993).

¾ inch downgraded stone chips had been used as coarse aggregate. Absorption capacity and moisture content of the coarse aggregate influence the property of the fresh concrete by altering the w/c cement ratio. Absorption capacity of the stone chips should not exceed 15-20% of its weight.

3.4   Cement

Cement is the binding material used for providing strength to the concrete. The properties of the cement depend on chemical constituents of the cement. The most important properties of the cement are hydration, setting, fineness and strength. Portland Composite Cement (CEM-II) had been used for construction of all samples. For Portland Composite Cement, the specification should conform to ASTM C595 and BDS EN 197-1:2003.

3.5 Reinforcement

Reinforcing bars are used to take high tension, compression and shear forces induced in the concrete member. Transfer of forces between concrete and the reinforcement depends on the bond strength between them. At present, all commercial reinforcing bars are deformed bars and have better bond performance with concrete than the plain reinforcing bars. Detail specification of reinforcement used for construction works are given in details in Section 5.3 of BNBC (1993). Φ12 mm, 10 mm, Φ8 mm of Grade 500 and Φ6 mm of 40 Grade steel had been used for model construction.

3.6 FRP Fiber System

Fiber Reinforced Polymers (FRP) are composite materials made of fibers in a polymeric resin. FRP systems include primer, putty fillers, saturating resins, adhesive and protective coatings. Primer is used to penetrate the concrete surface thus providing an improved adhesive bond for saturating resin or adhesive. Putty is used to provide a smooth surface by filling small surface voids to prevent bubbles forming up during curing of the saturating resins. Saturating resin is used to impregnate the reinforcing fibers, fix them in place and provide a shear load path to effectively transfer load between fibers. It also serves as the adhesive for wet layup systems, providing shear load path between the previously primed concrete substrate and the FRP systems. Adhesives are used to bond between the FRP laminate systems to the concrete substrate and to bond together multiple layers of FRP laminate. It provides a shear load path between the concrete substrate and the FRP reinforcing laminate. Zureick et al. 2001 suggested that the primer and the resin should only be applied when the ambient temperature is between 5º to 32º C, the relative humidity is less than 90%, the concrete surface temperature is more than 2ºC above the dew point and the concrete moisture content is no greater than 4%. They also suggested that the glass transition temperature of the resin should be at least 30ºC above the maximum operating temperature and that elapsed time between mixing and application of the first ply and between any two successive piles should be within a time period not exceeding the gel time of the resin. The protective coating is used to protect the bonded FRP reinforcement from potentially damaging environmental effects. Coatings are typically applied to the exterior surface of the cured FRP system after the adhesive or saturating resin has cured.
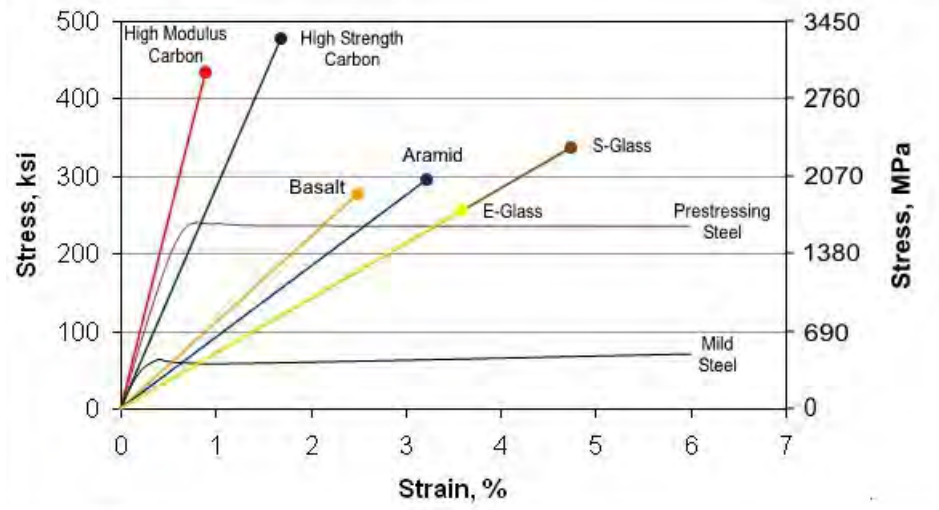
Fig. 3.2: Typical Stress –Strain Diagram of Steel and FRPs

FRPs are high strength materials but differ from steel in their material properties. Steel exhibits ideal elastic-plastic properties where FRPs show liner-elastic properties as shown in Fig. 3.2. This is an important design consideration for FRP materials. The basic fibers in the FRP systems are imbedded in a matrix and their arrangement can be unidirectional or bidirectional. They can take load basing on the direction of the arrangement of the fibers. FRP systems can be made of Glass, Aramid or Carbon and their properties and behavior differ widely based on the type of materials they are made of. Densities and co-efficient of thermal expansion of different FRP systems is shown in the Table 3.1 and Table 3.2.

Table 3.1: Typical Densities of FRP Materials gm/cm^3 (lb/ft^3) (ACI 440.2r-08)

Steel	GFRP	CFRP	AFRP
7.9	1.2 to 2.1	1.5 to 1.6	1.2 to 1.5
(490)	(75 to 130)	(90 to 100)	(75 to 90)

Table 3.2: Typical Coefficients of Thermal Expansion for FRP Materials (ACI 440.2r-08)

Direction	Coefficient of Thermal Expansion, x 10^{-6} /°C (x10^{-6} /°F)		
	GFRP	CFRP	AFRP
Longitudinal, α_L	6 to 10	-1 to 0	-6 to -2
	(3.3 to 5.6)	(-0.6 to 0)	(-3.3 to -1.1)
Transverse, α_T	19 to 23	22 to 50	60 to 80
	(10.4 to 12.6)	(12 to 27)	(33 to 44)

When loaded in direct tension, FRP materials do not exhibit any plastic behavior (yielding) before rupture. The tensile behavior of FRP materials consisting of one type of fiber material is characterized by a linearly elastic stress-strain relationship until failure, which is sudden and can be catastrophic. The tensile strength and stiffness of a FRP material is dependent on several factors. Because the fibers in a FRP material are the main load-carrying constituent, the type of fiber, the orientation of the fibers and the quantity of fibers primarily govern the tensile properties of the FRP material. Due to the primary role of the fibers and methods of application, the properties of an FRP repair system are sometimes reported based on the net-fiber area. In other instances, the reported properties are based on the gross-laminate area. The gross-laminate area of an FRP system is calculated using the total cross-sectional area of the cured FRP system, including all fibers and resin. The gross-laminate area is typically used for reporting pre-cured laminate properties where the cured thickness is constant and the relative proportion of fiber and resin is controlled. The net-fiber area of an FRP system is calculated using the known area of fiber, neglecting the total width and thickness of the cured system; thus, resin is excluded. The net- fiber area is typically used for reporting properties of wet layup systems that use manufactured fiber sheets and field-installed resins. The wet layup installation process leads to controlled fiber content and variable resin content. System properties reported using the gross- laminate area have higher relative thickness dimensions and lower relative strength and modulus values, whereas system properties reported using the net- fiber area have lower relative thickness dimensions and higher relative strength and modulus values. Regardless of the basis for the reported values, the load-carrying strength ($f_{fu}A_f$) and stiffness (A_fE_f) remain

constant. Properties reported based on the net- fiber area are not the properties of the bare fiber. The properties of an FRP system should be characterized as a composite, recognizing not just the material properties of the individual fibers but also the efficiency of the fiber-resin system, the fabric architecture and the method used to create the composite. The mechanical properties of all FRP systems, regardless of form, should be based on the testing of laminate samples with known fiber content. The tensile properties of some commercially available FRP strengthening systems are given in Table 3.3.

Table 3.3: Ultimate Tensile Strength of Some Commercially Available FRP Systems (ACI 440.2r-08)

Description of the FRP System (Fiber type/resin/fabric)	Fabric Weight (gm/m^3)	Ultimate Strength (KN/mm)†
General Purpose carbon/ epoxy unidirectional sheet	200	500
	400	620
High Strength carbon/ epoxy unidirectional sheet	230	320
	300	700
	300	960
High modulus carbon/ epoxy unidirectional sheet	300	600
General Purpose carbon/balanced sheet	300	180
E-glass/epoxy unidirectional sheet	900	720
	350	230
E-glass/balanced fabric	300	120
Aramid/epoxy unidirectional sheet	420	700
High Strength carbon/epoxy precured unidirectional sheet	2380††	3380†
E-glass /vinyl ester precured	1700††	1580

	unidirectional shell

† Ultimate Strength per unit width of sheet of fabrics
††Precured laminate weight

The CFRP Fabrics system is comprised of the CFRP fabrics, epoxy sealer cum primer and high build epoxy saturant. The system can be protected by a polyurethane top coat in case of atmospherically exposed structure. For this research, polyurethane top coat was not used.
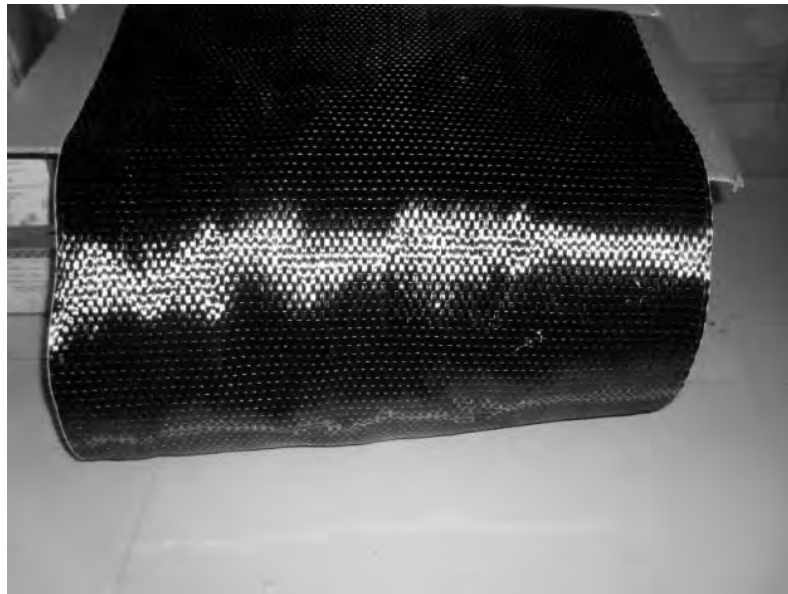
Fig. 3.3: CFRP Fabrics

3.6.1   CFRP Fabrics

'Nitowrap EP (CF450)' of FOSROC Constructive Solution was used as CFRP fabrics in this experiment. The properties of the CFRP fabrics as per supplied catalogue (attached in Appendix-A) are as follows:

Fiber Orientation:	Unidirectional
Weight of Fiber:	450g/m^2
Fiber Thickness:	0.25-0.30 mm
Ultimate Elongation:	1.5%
Primary Fiber Tensile Strength:	4300 N/mm^2
Tensile Modulus:	240x 10^3 N/mm^2

3.6.2   CFRP Fabric Primer

"Nitowrap 30, Primer" of FOSROC Constructive Solution was used as primer with the CFRP Fabrics in this experiment. The properties of the primer are as follows:

Density:	1.14 gm/cc
Pot Life:	25 min at 27ºC
WFT:	100 Microns
DFT:	100 Microns
Indicative Coverage per coat/liter:	8.0-10.0 m^2
Full Cure:	7 days

3.6.3   CFRP Fabric Saturant

A high built epoxy saturant "Nitowrap 410" of FOSROC Constructive Solution was used with the CFRP Fabrics in this experiment. The properties of the saturant are as follows:

Color:	Pale yellow to amber
Application Temperature:	15ºC to 40ºC
Viscosity:	Thixotropic
Density:	1.25-1.26 gm/cc
Pot life:	2 hours at 30º C
WFT:	250 Microns
DFT:	250 Microns
Indicative Coverage per coat/liter:	3.5-4.0 m^2
Cure Time:	5 days at 30ºC

3.6.4   Application instruction

Concrete substrate should be free from oil residues, demoulding agents, curing compounds, grout holes and protrusions. If the substrate exhibits any damage due corrosion then substrate should be repaired before application of CFRP. Structural damage also has to be repaired before applying FRP wrapping. All depressions, imperfections etc have to be repaired by using epoxy putty. The base and the hardener

are emptied into a suitable container and mixed through for at least 3 minutes. Mechanical mixing using a heavy duty slow speed (300-500 rpm) drill, fitted with a mixing paddle is recommended by the manufacturer. Epoxy primer is applied over the prepared and cleaned surface by brush and should be allowed for drying for about 24 hours before application of saturant.

CHAPTER FOUR

MODEL PREPARATION AND EXPERINTAL PROGRAMME

4.1   General

The objectives of this research are to study the behavior of the RC exterior beam-column joints which lack in shear reinforcement, behavior and ductility of the retrofitted joints and identify suitable methods of retrofitting them by FRPs. This experimental research needed a methodological approach to attain the research objectives. It was needed to develop a thorough knowledge on the ductility of the structure, behavior of the structure under seismic loading, current retrofitting methods for changing the global and member behavior of the structure, material properties and their interaction with each other. In this study the joints were retrofitted by wrapping beams and columns with FRP in the joint region. All the models were subjected to constant axial and incremental cyclic loading. The deflection of the column, beam and rotation of the joints were measured to study their behavior.

4.2   Model Selection and Preparation

The models had been selected considering a full scale six storied RC Frame Structured Building as shown in Fig. 4.1. The building was analyzed as per BNBC (1993). An exterior joint at the mid height of the structure had been selected for the experimental program as shown in Fig.4.2. Considering the existing laboratory set up an half scale model had been selected. Dimensions of the as built models are shown through Fig. 4.3 to 4.4.

Total three models were constructed for the experiment. All the models had identical dimensions. The cross section area of the column and beam were 225 mm x 225 mm and 150 mm x 225 mm, respectively. Geometry of sample and reinforcement details are shown in Fig. 4.3 and Fig. 4.4. There were no tie bar (shear reinforcement) at the joints of Model-C2 & Model-F and two tie bars were provided at the joint of Model-C1. Neither beams nor the columns had any lap joint. Tie and stirrups had standard 135º hook as per BNBC (1993). The samples were constructed from same concrete batches.
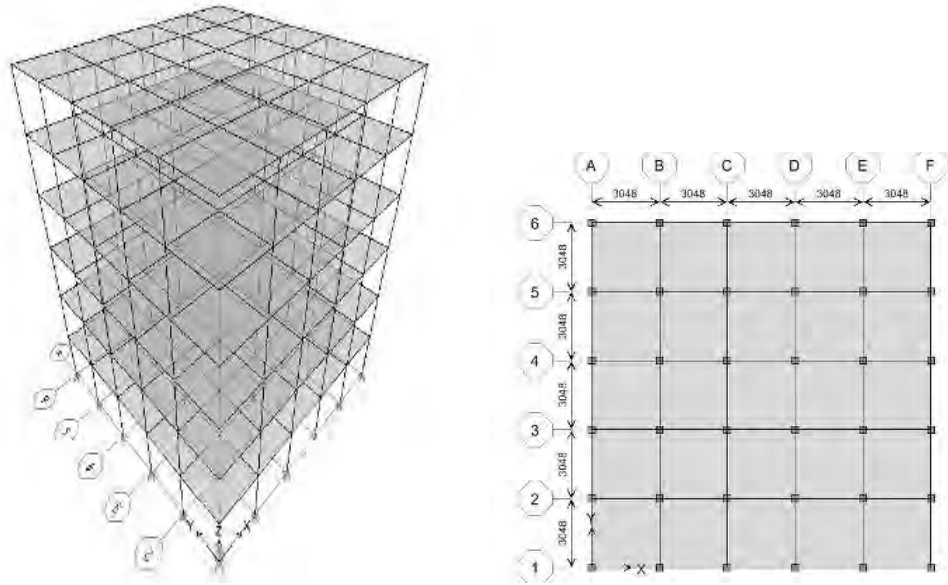
Fig. 4.1: 3D and Plan View of the Structure
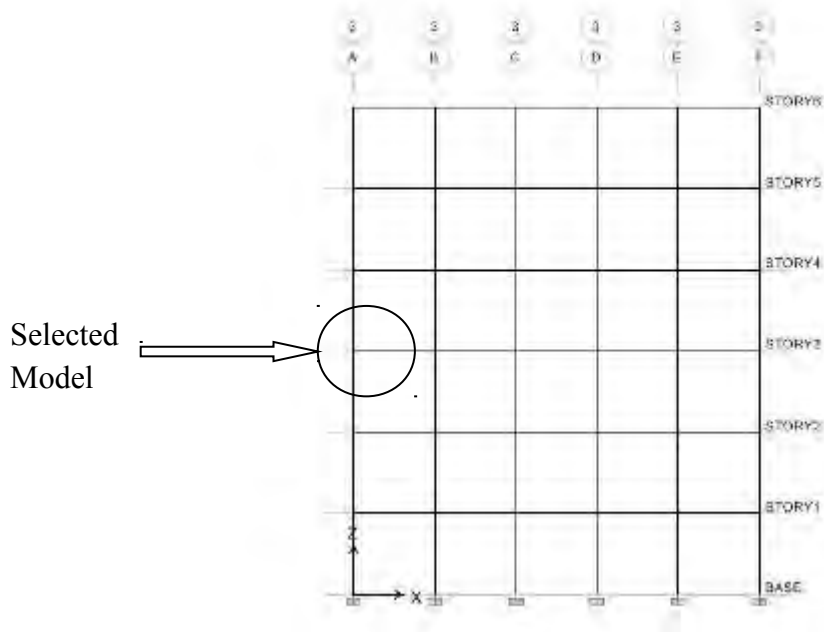

Selected Model

Fig. 4.2: Selection of the Test Model

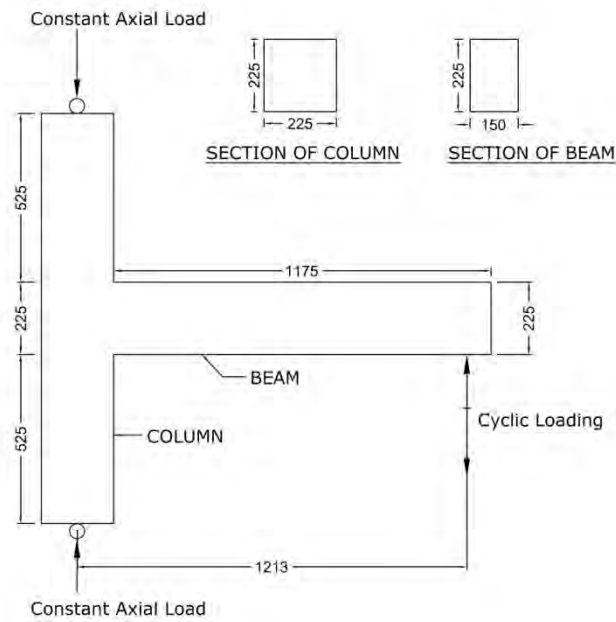All dimension are in mm where not mentioned

Fig. 4.3: Dimensions of Beams and Columns

No Shear Reinforcement except Model-C1

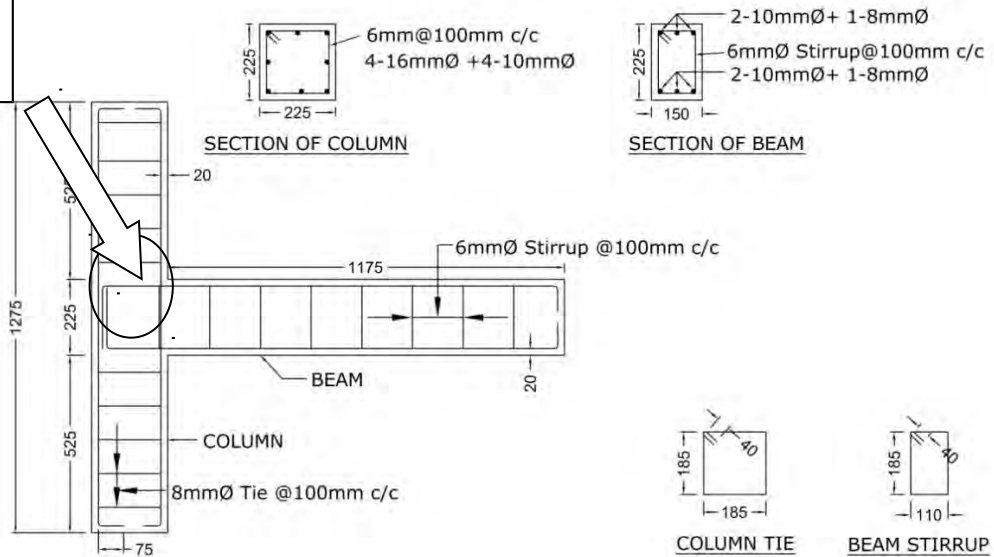All dimension are in mm where not mentioned

Fig. 4.4: Reinforcement Details of Beams and Columns

The form works for casting the models were prepared by woods and plywood. Total three formwork (Fig. 4.5) models were prepared for casting.

Fig. 4.5: Preparation of Formwork

All parts of model (column & beams) were cast together. Water content of fresh concrete had been controlled by slump value to ensure better workability. Slump value varied between 50-75 mm. W/C ratios of the concrete batch were 0.5. The models were mechanically compacted. The models were cured by wet hessian cloth for 28 days before retrofitting the joints. To minimize the loss of moisture from the models, the form works (Shuttering) were kept with the poured concrete for 28 days. Concrete strength was measured by Cylinder tests. The Cylinder test result at 28th days is 38.42 MPa (detail shown in Table: A2, Appendix -A).

4.3 Strengthening the Joints by CFRP fabrics

Model-F is wrapped by two layers of CFRP fabrics as shown in Fig. 4.6 & 4.7. One layer is on each side of column and U-shaped sheet on the beam. Second layer is provided by wrapping one layers of 150 mm wide sheets at the ends of three members (two columns, one beam) meeting at the joint to improve the anchorage of the first layer sheets.
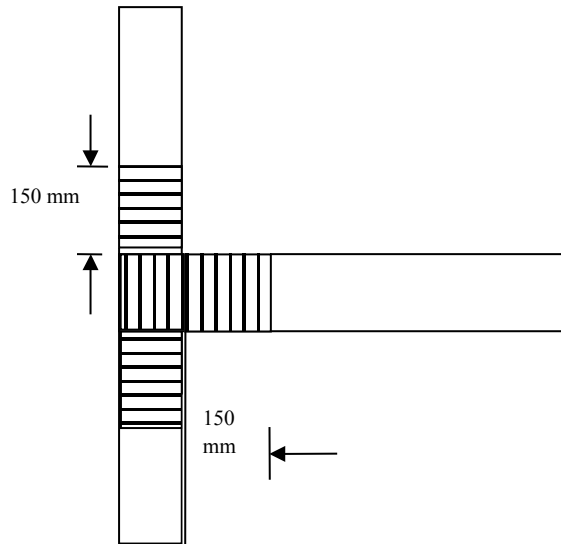
Fig. 4.6: Details of Wrapping by CFRP Fabrics

4.3.1 Surface preparation

CFRP wraps is not recommended to use for inside corners and minimum 12 mm radius should be provided for confinement by FRPs. The beams and column sides were rounded to provide 12 mm radius curvature. The surface of the beams and columns were smoothened by grinding machine and cleaned thoroughly by brush before applying Primer.

4.3.2 Application of epoxy primer

Hardener and Base (1:2 ratios) were mixed thoroughly for 3 minutes before applying on the prepared surface. This epoxy primer was applied by using a brush and dried for 2 hours before applying the saturant.

4.3.3 Strengthening by FRP fabrics

At first, the CFRP fabrics were cut into required size. The hardener and the base (1:2 ratios) of the saturant were mixed and applied over the primed surface. Then the first layer of CFRP fabric had been pressed on to the saturant applied area by hand first and then was pressed by a surface roller to remove air bubbles. After 30 minutes another

coat of saturant was applied over the carbon fabrics. Immediately second layer of CFRP fabrics were pressed on the saturant. Again after 30 minutes later another coat of saturant was applied over the fabrics. The sample was allowed to cure for 7 days in open air.

Fig. 4.7: CFRP Fabrics wrapping

4.4   Experimental Set Up

The experiment had been carried out in Concrete and Strength of Materials Laboratory of BUET. Attempts were taken to avoid any potential damages during lifting, transporting and loading of the models. The models had been lifted by series of pulleys. The models were placed on a steel base plate which had the arrangement of column seat. The base plate was intended to allow column rotation. The base plate was fixed on a steel beam which was fixed with the concrete floor as shown in Fig. 4.8(a) and Fig. 4.8(b). The top portions of the columns were supported by two horizontal beams of the steel frame to resist against any horizontal movement while allowing the column rotation. Details of the steel frames are given in Appendix C. They were fixed at both side of the column to arrest any horizontal movement of the column. A hydraulic jack was set to provide axial load on the top of the column. And a manually operated hydraulic jacks were used to provide cyclic loading at the tip of the beams. Steel plates were used above the piston of both hydraulic jacks to avoid local failure. Experimental set up is shown in Fig. 4.8(b).

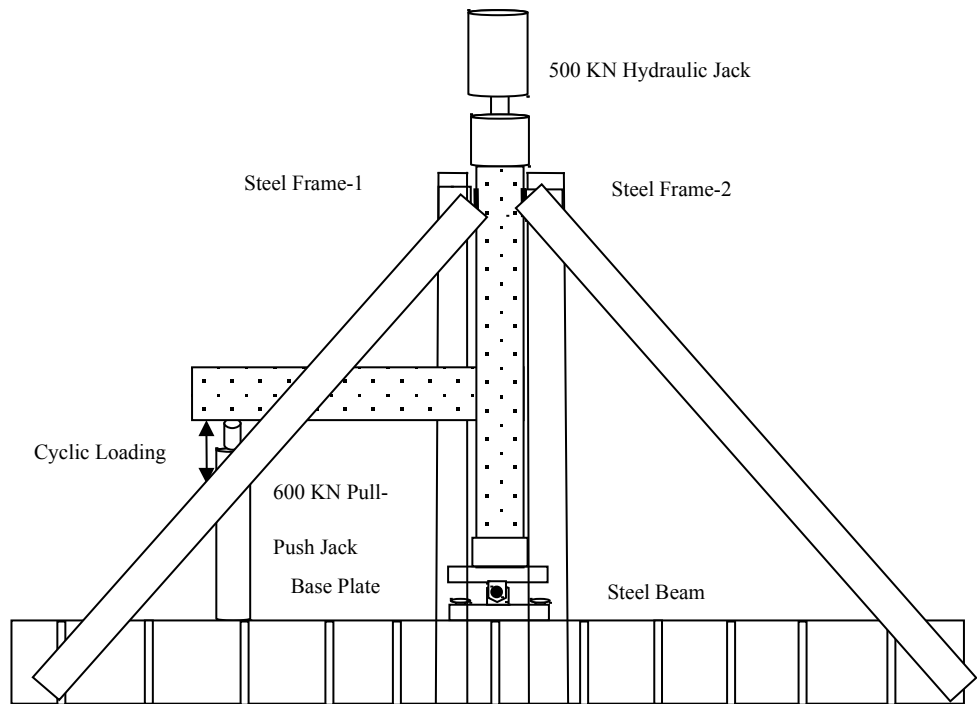**Fig. 4.8(a): Experimental Set Up**

Fig. 4.8(b): Experimental Set Up

Total three dial gauges were used to measure the deflection of the beam and columns. First two dial gauges were set near the tip and at the mid-span of beam. Another dial

gauges were set at below the top of column. The location of the dial gauges are shown in Fig. 4.9.
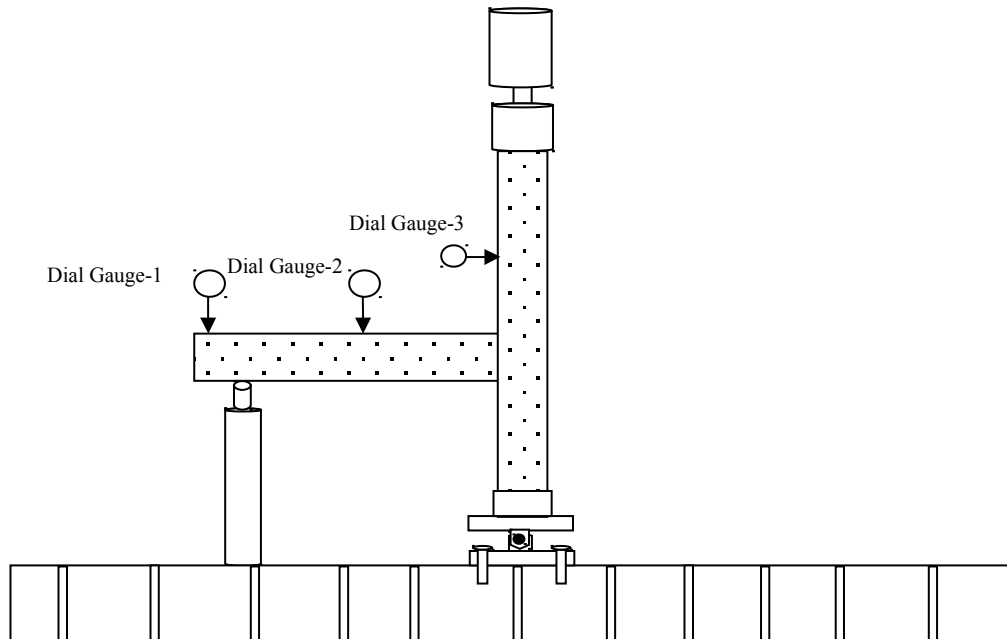
Fig. 4.9: Location of the Dial Gauges

Video extensometer was used to measure the rotation of the beam and column joint. Video extensometer had been placed much closed to the joint due to space constrain and location of the steel frame. "+" marking on the joint, as shown in the Fig. 4.10 and Fig. 4.11, had been used as the target to measure the beam and column joint rotation. The mark on the wooden plank was used to measure the absolute rotation of the specified target.
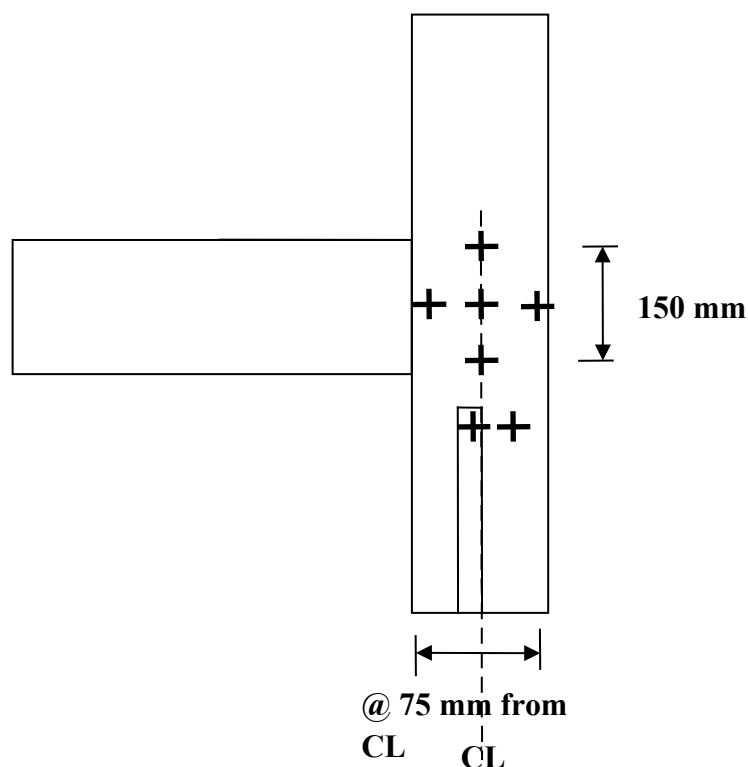
Fig. 4.10: Schematic Diagram of Target for Video Extensometer
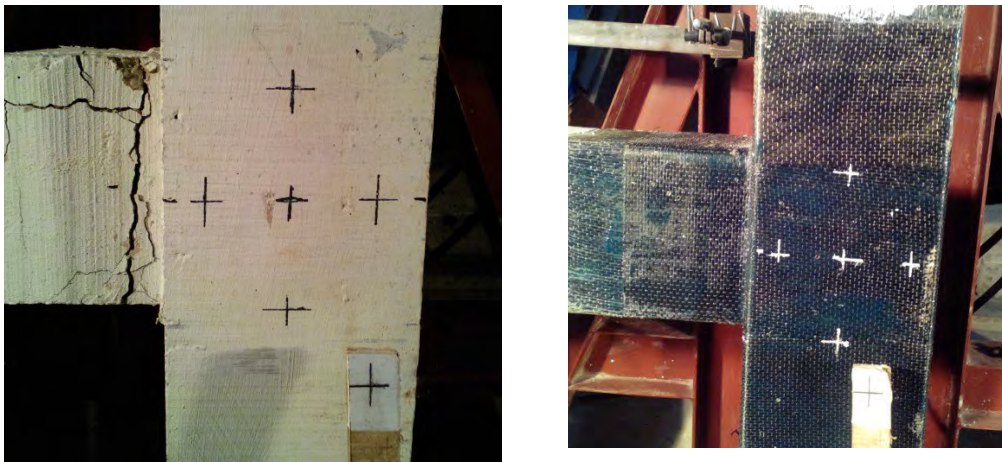
Fig. 4.11 : Registration of Target for Video Extenso Meter

4.5   Load Selection

The strengths of BC joints are influenced by the effective confinement. Column axial load increase the confinement. The samples were made from same concrete batch as such there concrete strength had been same. To understand the behavior of all joints under identical condition 10% of the column capacity ($0.1f_c'A_g$) was provided as the axial load. Axial load had been constant throughout the experiment. Axial loads on all the model was fixed as 127 kN.

The static cyclic loading had been provided by a manually operated hydraulic jack. The loading and the unloading were manually controlled. A cycle with upward load from the hydraulic jack is considered as forward loading and vice versa is considered as reverse loading.

The load had been controlled by measuring the beam deflection of the beam edge. 0.25%, 0.50%, 1% and 2% of the beam deflection had been selected to control the load. 5 kN load had been applied while loading and unloading. However, as the jacks were manually operated, unloading could not be maintained at the same rate. The planned load cycle are shown in Fig. 4.12 (Kibria, 2014).
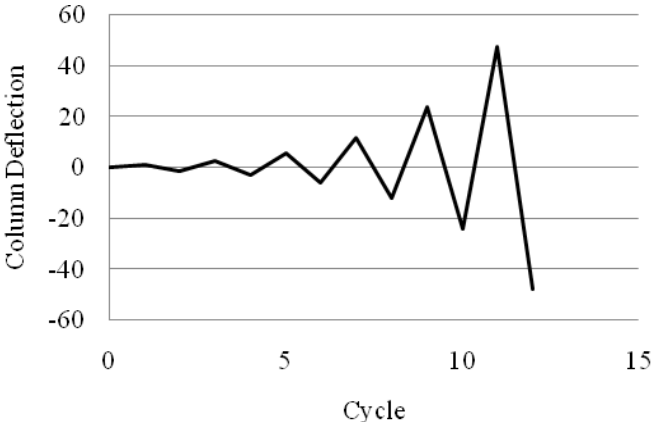

Fig. 4.12: Loading Cycle of the Experiment

CHAPTER FIVE
EXPERIMENTAL RESULTS AND DISCUSSIONS

5.1   General

In this chapter the qualitative and quantitative analysis and results of the experiments will be presented. All three Models were subjected to constant axial load throughout test and incremental cyclic loading. Failure and cracking pattern of the samples are represented by photographs taken throughout the experiment in qualitative analysis. Dial Gauges and Video Extensometer were used to measure the deflection and rotation of the beams, columns and joints. Quantitative results are represented by tables, graphs and charts.

5.2   Failure Pattern of Samples

The cracking and failure pattern of the samples were different as their shear reinforcement and joint retrofitting strategies had been different. Behavior of the samples is discussed in the subsequent paragraphs.

5.2.1   Behavior of Model-C1

The cracks and the corresponding loading are shown through Fig. 5.1 to 5.4. First joint crack initiated on beam in second forward cycle (Fig. 5.1) when the applied moment was 17.88 kN-m. Two more cracks appeared during cycle -3 on beam and joint face and the earlier crack widen to 1.3 mm. Applied moment at this point was 35.77 kN-m (Fig. 5.2). Shear cracked appeared at column face of joint at cycle-3 and thickened to 1.15 mm at cycle-4 forward cycle when the applied moment reduced to 22.36 kN-m (Fig. 5.3). After reverse cycle of cycle-4 cracks formed earlier thickened to 1.75 mm and Concrete, at the face of the joint, from both upper and lower columns, completely disintegrated (Fig. 5.4). Some small flexural cracks were marked on the beam at this stage. The test had been discontinued when the dial gauge reached its maximum capacity.
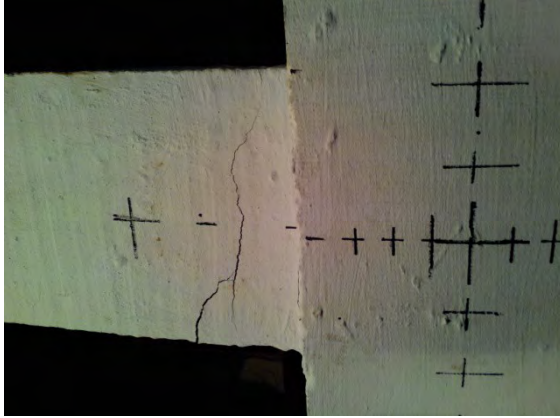
Fig. 5.1: Appearance of First Joint Crack
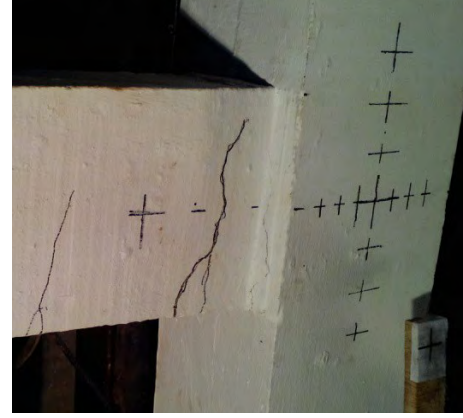
Fig. 5.2: Appearance of Second and Third Joint Crack

Fig. 5.3 : Shear Crack at Column Joint Face

Fig. 5.4: Shear Crack at Beam Face

5.2.2   Behavior of Model-C2

The cracks and the corresponding loading are shown through Fig. 5.5 to 5.8. First flexural cracks initiated during the third reverse cycle when the beam deflected 28 mm by 29.1 kN applied load. Shear cracks appeared at upper portion of beam at joint during the 4th forward cycle as shown in Fig. 5.6 with corresponding applied moment of 33.6 kN-m. At 4th reverse cycle the earlier formed two cracks thickened to 10 mm and 0.1 mm respectively and new flexural crack formed as shown in Fig. 5.08. Concrete from both top and bottom started to spall out at 5th reverse cycle as shown in Fig. 5.8. The test discontinued as the jack had reached its maximum capacity.
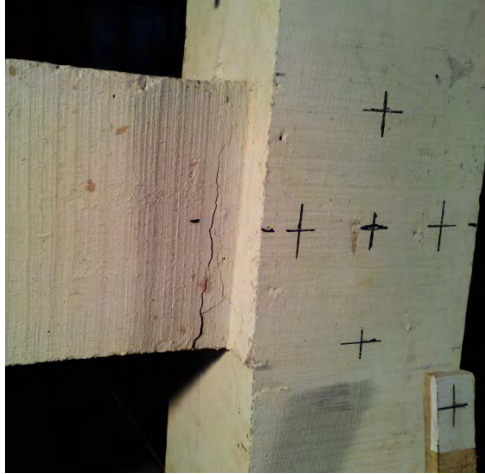
Fig. 5.5: Appearance of First Flexural Crack

Fig. 5.6: Appearance of Shear Crack

Fig. 5.7: Appearance of Second Flexural Crack

Fig. 5.8: Disintegrate the concrete

5.2.3 Behavior of Model-F

The cracks and the corresponding loading are shown through Fig. 5.9 to 5.11. Several flexural cracks appeared from the midsection of the beam to near the joint third forward cycle when beam deflection was 17.7 mm and applied load was 24.2 kN. De-bonding of FRP was observed at bottom corner of beam of Joint during 5th forward cycle when applied moment was 37.8 kN-m. De-bonding also occur at top corner of beam at 5th reverse cycle when applied moment was 42 kN-m.

Fig. 5.9: Flexural Cracks on the Beam   Fig. 5.10: De-bonding of FRP at bottom corner
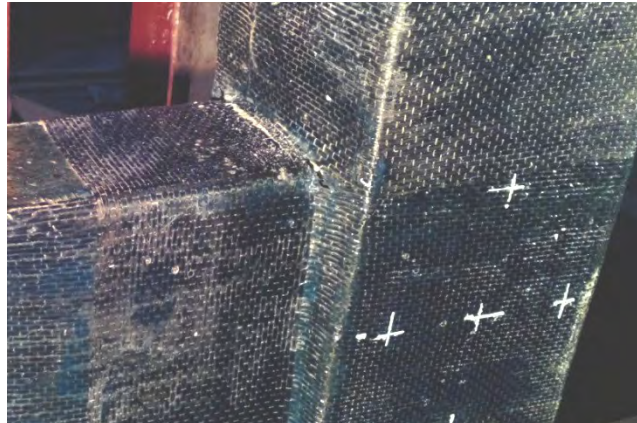
Fig. 5.11: De-bonding of FRP at Top Corner of Beam

5.3   Load Deflection Response

5.3.1.   Load deflection behavior of beam

Deflections of all the samples were measured by three dial gauges. The location of the dial gauges had been described in Chapter Four. Video Extensometer had been used to measure the joint and column rotations. The test continued till the left dial gauges reached optimum deflection or the jacks reached their maximum lift capacity.

Load vs. deflection curves have been drawn for all the models to investigate their structural behaviour and to compare the retrofitted model with the control model as shown in Figure 5.12 to Figure 5.19. All these curves have been drawn taking the maximum deflections from each cycle with their corresponding loads. Detailed data of maximum deflections from each cycle with their corresponding loads are given in Table B.1 in Appendix-B. Plastic strength of the beam had been calculated based on the theory of beam and plotted with their load-deflection curve to compare their behavior. A detail of the calculation is given in Table B.6 in Appendix-B.
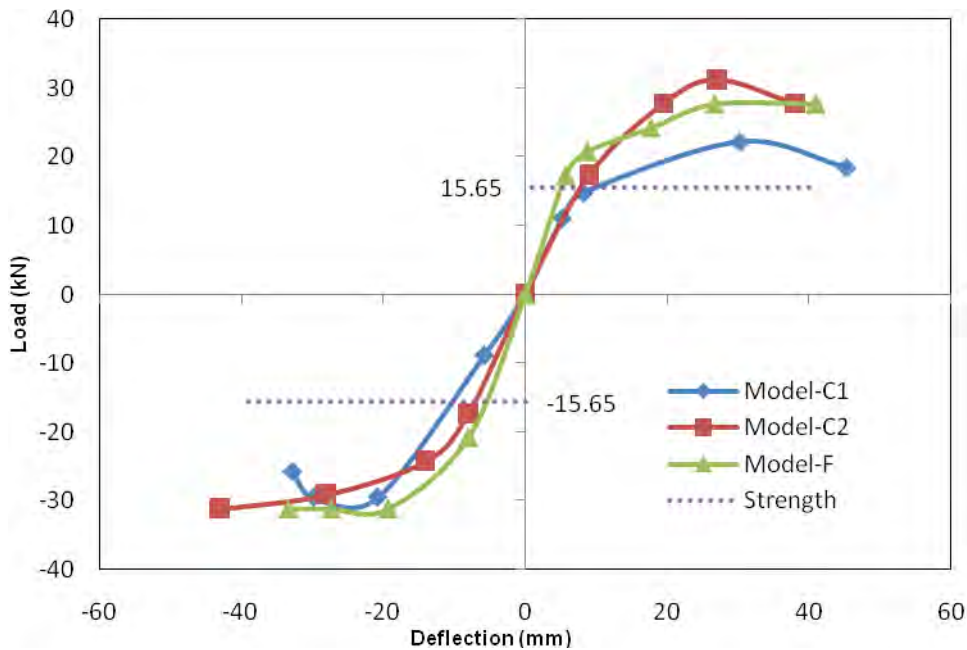
Fig. 5.12: Load Deflection Response of Beams

By analyzing the Fig. 5.12 it is found that load deflection behavior of beams for all the models are almost similar. The reason is that, beam flexural failure was initiated before joint shear failure. Highest possible shear force may develop at joint before flexural failure of beam is 88.6 kN, which is much smaller than the shear strength capacity of the joint (260.4 kN). Detail of these shear stress calculations are given in Appendix B Table B.7 & B.8.

All the models yielded at higher loading than the load corresponding to its plastic yield strength in both forward and reverse loading. Model-C2 and Model-F exhibited better strength in forward loading whereas more ductility in reverse loading than Model-C1.

Load-Deflection behaviors of beams are illustrated by hysteresis loops through Fig. 5.13 to 5.15.

Fig. 5.13: Load-Deflection Response of Beam of Model-C1
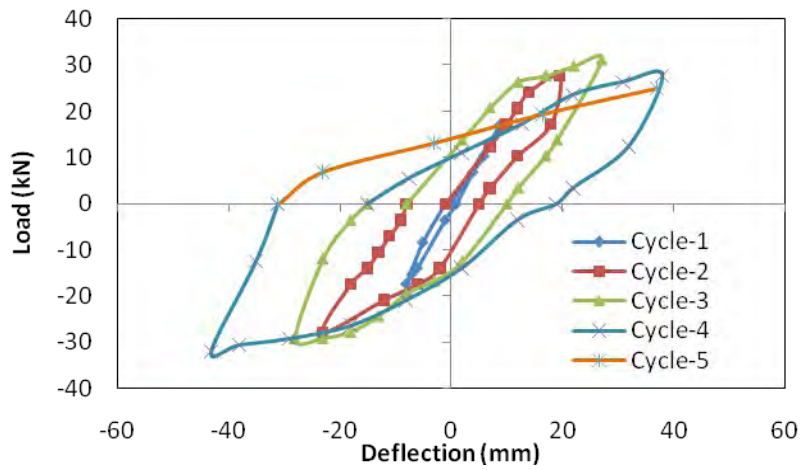
Fig. 5.14: Load-Deflection Response of Beam of Model-C2
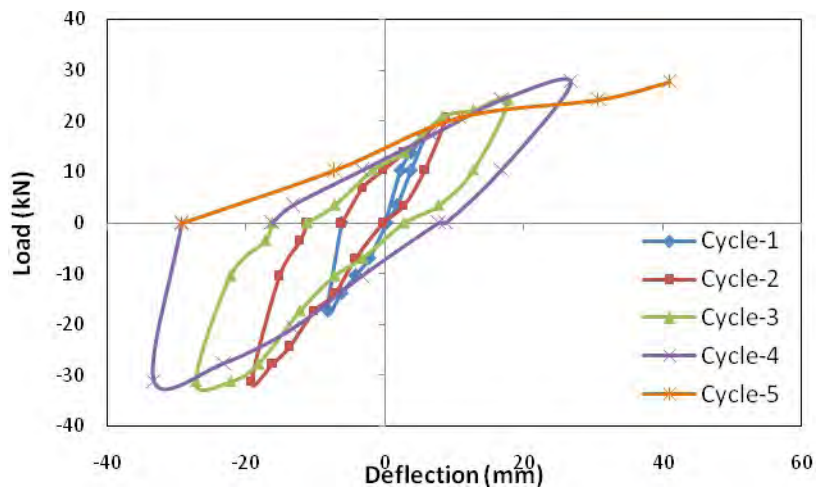
Fig. 5.15: Load-Deflection Response of Beam of Model-F

By analyzing the hysteresis loops of the load-deflection, it is found that, within the elastic limit, all the models have non-degrading curve. But in subsequent circles, the loops exhibit stiffness degradation.

Total energy absorption by the joint has been found by integrating the area under the hysteresis loop of every cycle of load-deflection curve (shown in Table B.4, Appendix – B). Absorption of energy by the retrofitted model (Model-F) is 21% higher than the control model C2 and 170% higher than the control model C1 as shown in Fig 5.16.
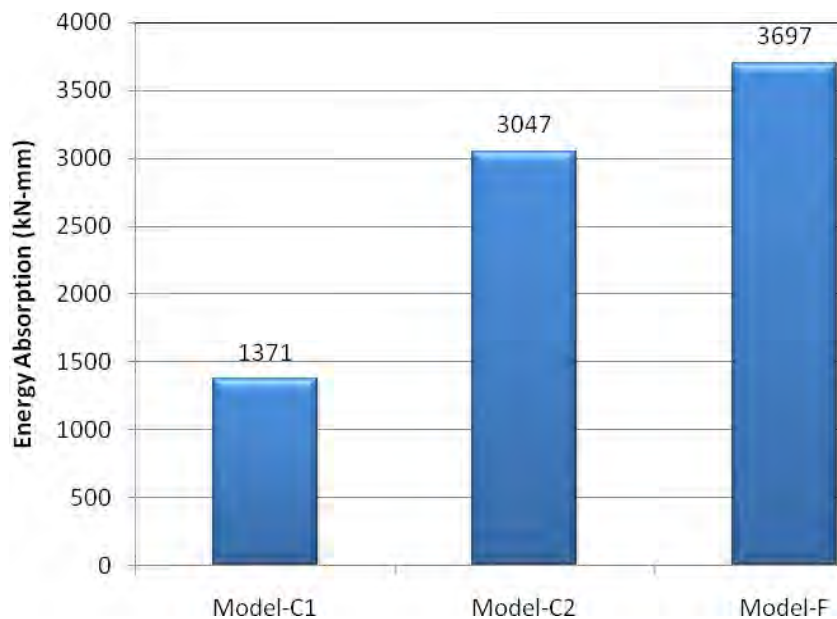
Fig. 5.16: Energy Absorption of Joint

Secant stiffness is defined as the ratio of the strength to the maximum displacement. Secant stiffness of the beams for each load-deflection cycle is measured by considering the maximum load and deflection of both forward and reverse loading.
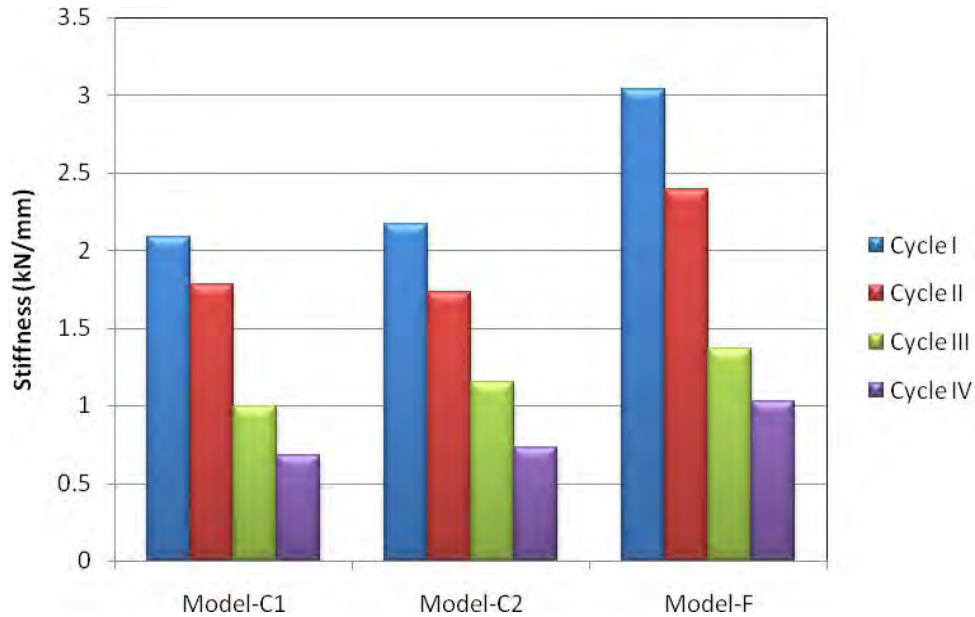
Fig. 5.17 : Stiffness of Beams

It is found that Model-C2 exhibits slightly higher stiffness than Model-C1 and Model-F shows highest stiffness in every cycle of loading. Beam stiffness decreases in each subsequent cycle as shown in Fig. 5.17. The rate of loosing stiffness in subsequent cycles indicates the collapse behavior of the member.

5.3.2 Load deflection behavior of column

Load deflection response of columns is presented through Fig. 5.18 to 5.22. Detailed data of maximum deflection from each cycle with their corresponding shear force are given in Table B.2. Column of Model-F experienced enhanced column shear capacity. Column of Model-F experienced excess column shear force while deflecting less in forward loading and exhibits more ductile behavior with high column shear force in reverse loading than the column of Model-C1 & Model-C2. In all the cases, the columns experienced low shear than their theoretical yield strength because the column shear had been measured indirectly from the load applied at the tip of the beam.
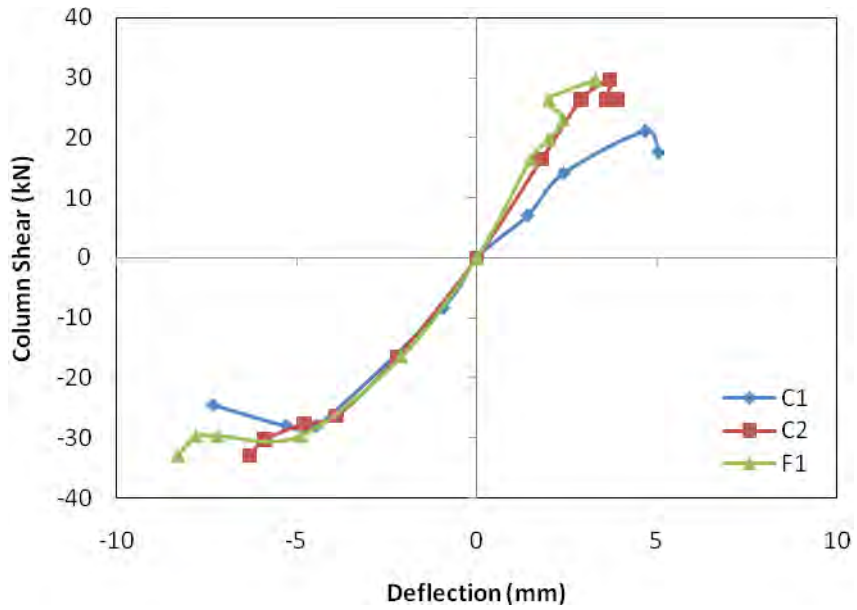
Fig. 5.18: Load Deflection Response of Columns

The behavior of the columns can be analyzed by the load-deflection hysteresis loops plotted for each cycle. Hysteresis loops for the columns are illustrated through Fig. 5.19 to 5.21.
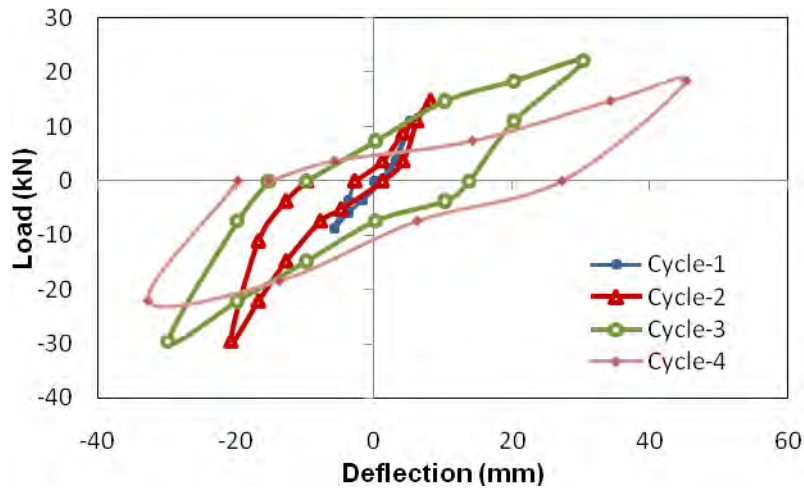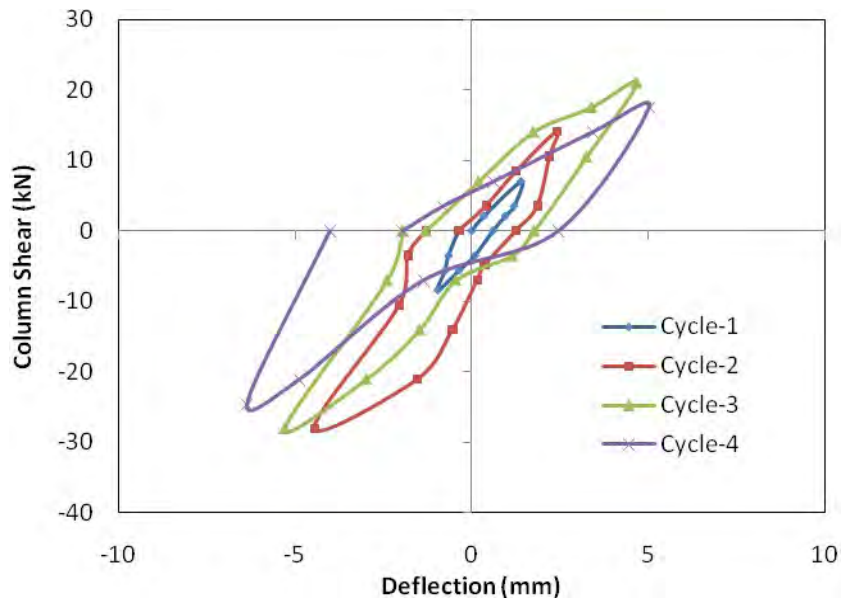

Fig. 5.19: Load-Deflection Response of Column of C1
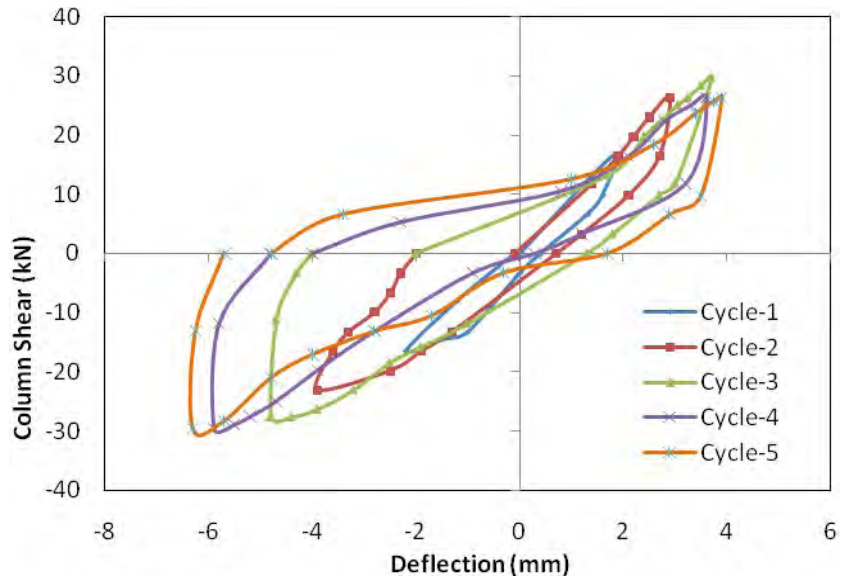
Fig. 5.20: Load-Deflection Response of Column of C2
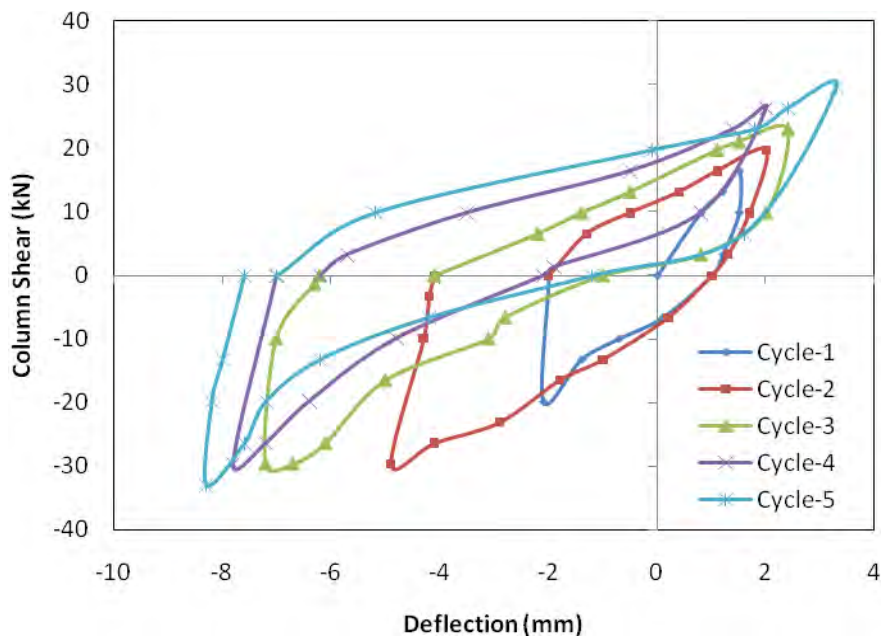
Fig. 5.21: Load-Deflection Response of Column of Model-F

Column secant stiffness for each cycle is measured by considering maximum applied moment against maximum deflection. The computed stiffness are illustrated by Fig. 5.24 and Fig. 5.25.
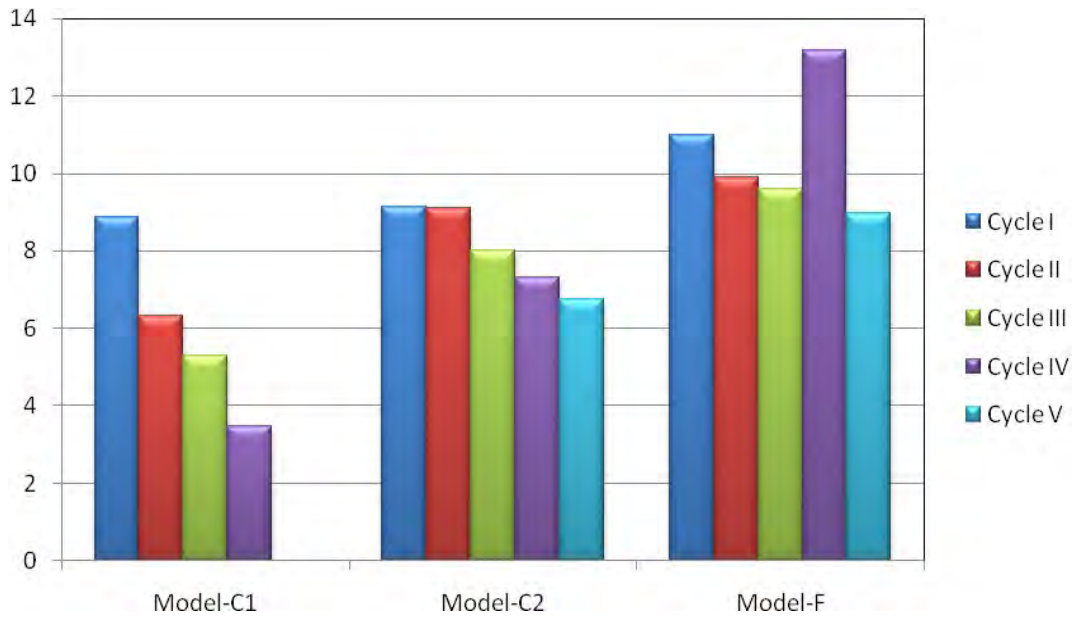
Fig. 5.22: Column Stiffness

The slopes and the secant stiffness of the column decreased with the commencement of cycles. The column shear had been measured indirectly from the load applied at the tip of the beam. Upon failure (at cycle IV), beams were unable to transfer load on the column. This led to increased column shear without deflection resulting in higher slope and stiffness in subsequent cycles.

5.3.3 Load deflection behavior of joint

Rotation experiences by the joints in each cycle depend on the magnitude of the applied moment. Rotations of the beams and columns at the joint against corresponding loading (applied moment) were measured and evaluated by Video Extensometer. Video Extensometer gave output as Time vs. Rotation and Time vs. Load had been recorded manually. Maximum load and corresponding rotation had been found by analyzing the computer output. Details of the applied moment vs. rotation of the joints are given in Table B.3 of Appendix B.

Unfortunately, rotational data of model-C1 was not recorded by Video Extensometer due to instrumental error. For that reason, the rotational behaviors of Model-C2 and Model-F have been compared only.

Applied maximum moment and corresponding beam joint rotations are shown through Fig. 5.23 to Fig 5.26. Joint of Model-C2 rotated more than Model-F against same

Moment in forward cycle whereas the Model-F joint showed more ductility than Model-C2 in reverse cycle.
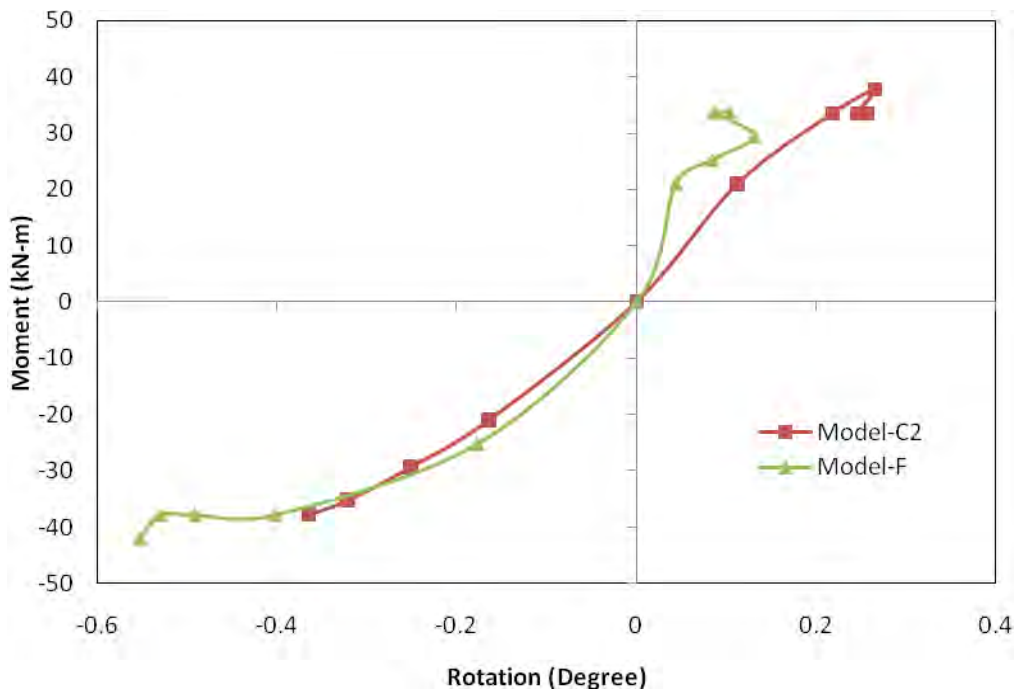
Fig. 5.23: Applied Moment vs. Rotation of Joint

Hysteresis loops of column and beam joints are shown through Fig. 5.24 to Fig. 5.25.
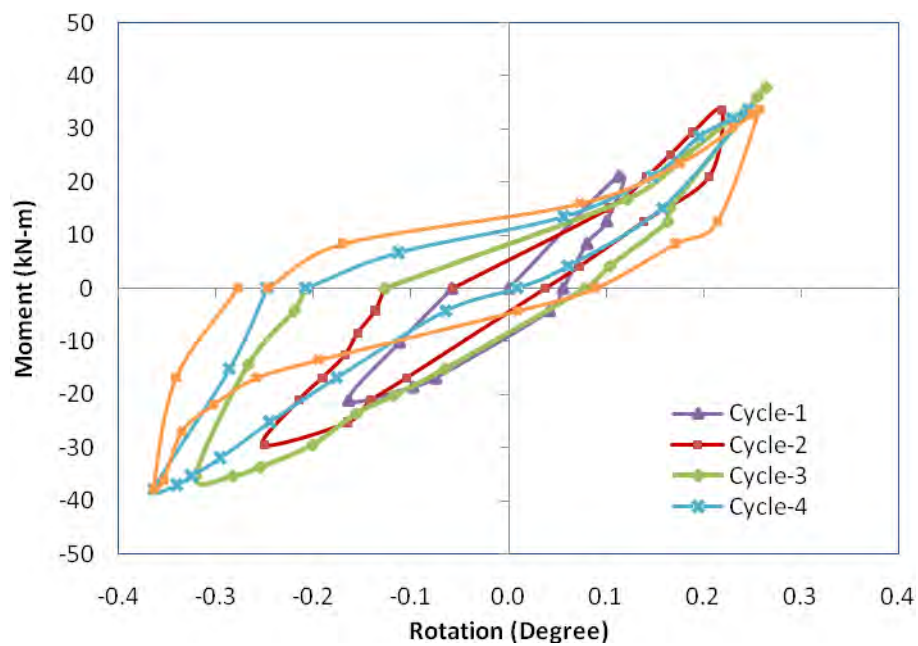
Fig. 5.24: Rotation of Joint of Model-C2
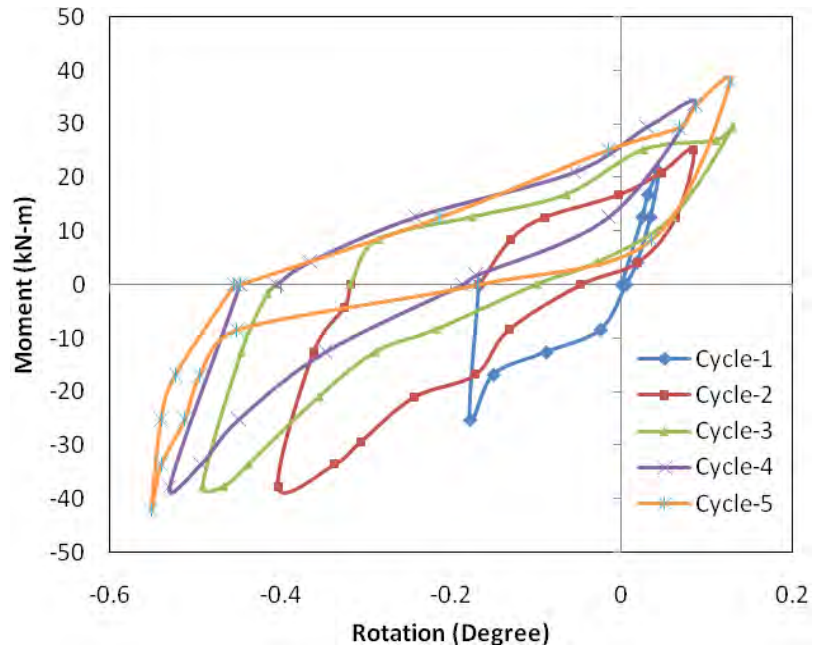
Fig. 5.25: Rotation of Beam Joint of Model-F

Rotational ductility is found by adding the highest amount of rotation occurred in forward and reverse loading. Detail calculations of rotational ductility of the joint are given in Table B.9 in Appendix-B. Retrofitted model-F shows 8.58% more rotational ductility than control model-C2 as shown in Fig. 5.26.
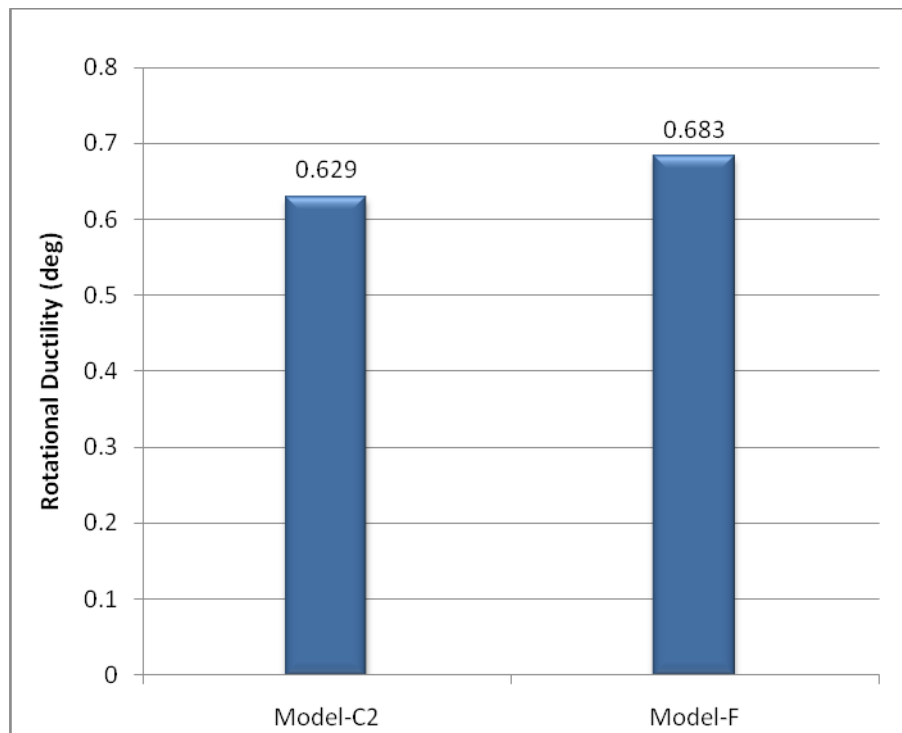
Fig. 5.26: Rotational Ductility of Joint

Rotational stiffness means the moment required to cause unit rotation. High stiffness means high resistance to rotation. Rotational Stiffness of the joint is computed as the ratio of the applied maximum moment against the maximum rotation.

Rotational stiffness is illustrated by Fig. 5.27. The rotational stiffness joint decreased with the commencement of the cycles for all samples. Joint of Model-F exhibited high rotational stiffness compared to the joint of Model-C2.
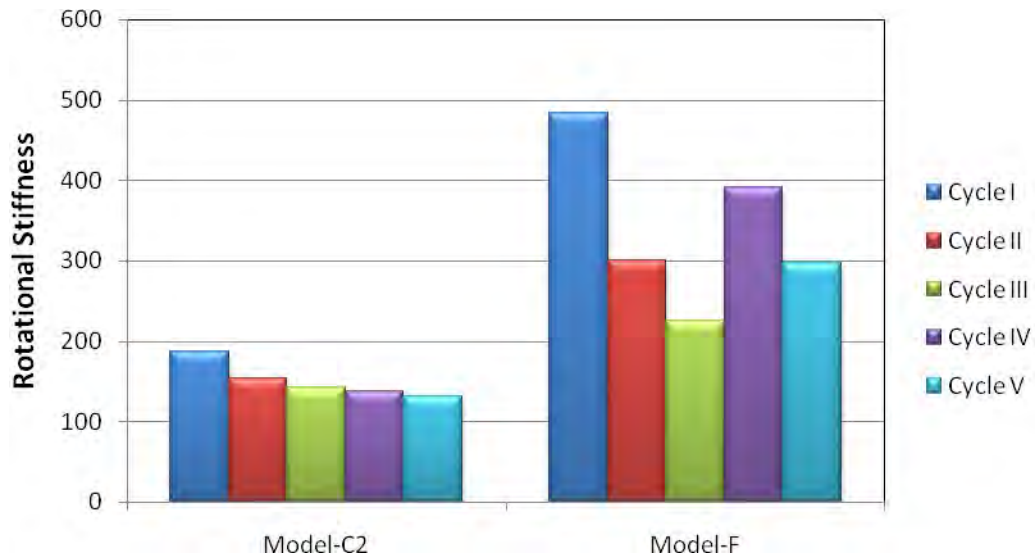
Fig. 5.27: Joint Rotational Stiffness

The rotational stiffness of the joint decreased with the commencement of cycles. The joint rotation had been measured indirectly from the load applied at the tip of the beam. Upon failure of the beam (at cycle IV), it was unable to transfer moment to the joint. This led to increased moment without further rotation of joint resulting in higher stiffness in subsequent cycles.

5.4   Comparison between Exterior and Interior Joint behavior

In this section, various properties of FRP strengthened interior joint from M. Sc. thesis of Kibria (2014) have been compared with of FRP strengthened exterior joint of this thesis paper. Kibria (2014) has considered three FRP fabrics wrapping samples varying in concrete strength only in his research. Out of them, the sample with concrete strength of 33.77 MPa (designated as Fabric-3) has been compared with Model-F (concrete strength 38.42 MPa) of this paper.

5.4.1   Initial stiffness of Joints

The initial stiffness of both exterior and interior joints has been compared with their control model in Fig. 5.28. It is observed that the initial stiffness of FRP strengthened exterior joint increases 40.3% than control model whereas for interior joint this increment is 27.6%.
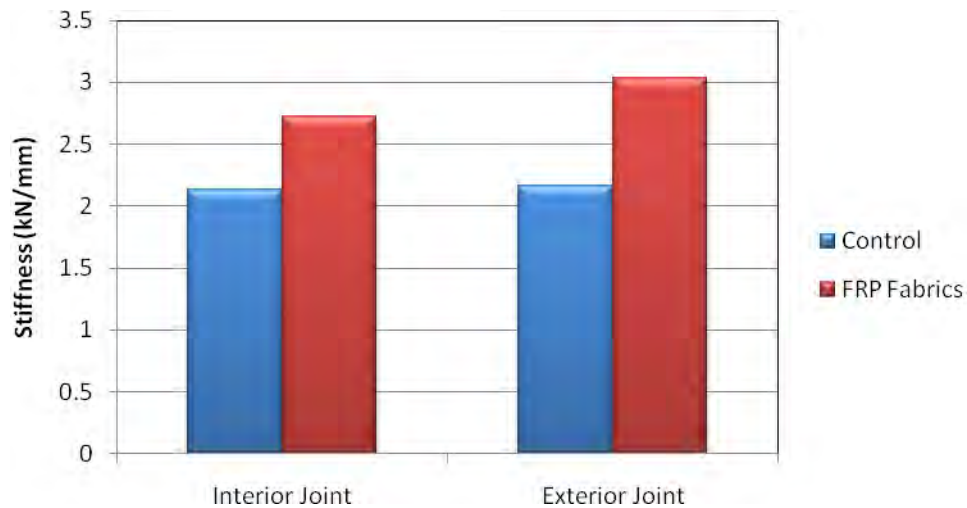
Fig. 5.28: Initial Stiffness of Interior and Exterior Joint

5.4.2   Stiffness degradation of Joints

Percentages of stiffness degradation from cycle-I to cycle-IV for both exterior and interior joints have been compared in Fig. 5.29. FRP retrofitted exterior joint model experienced 65.84% stiffness degradation where interior joint model experienced 70.18%.
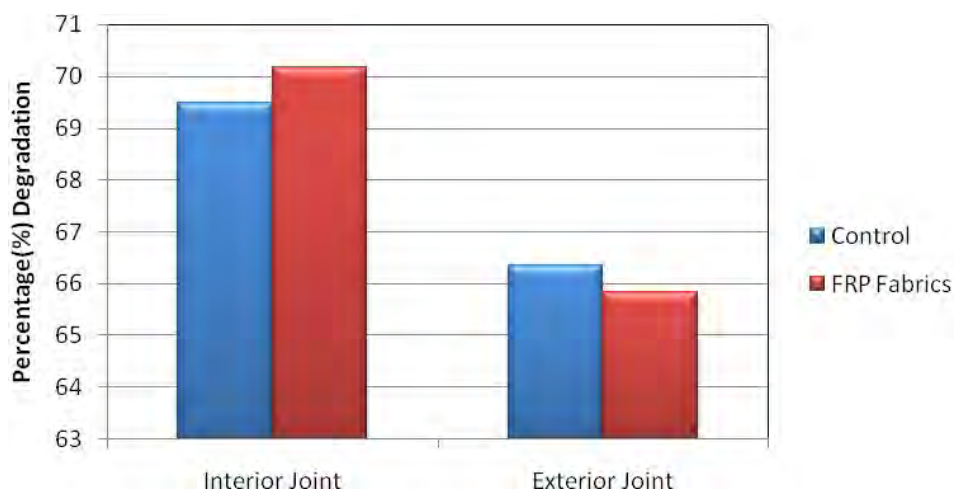
Fig. 5.29: Stiffness Degradation of Interior and Exterior Joint

CHAPTER SIX
CONCLUSION

6.1 General

The objectives of this study were to investigate the behavior of the exterior beam column joints retrofitted by CFRP Fabrics with a view to bring out some conclusions to recommend suitable methods of retrofitting the exterior BC joints. To achieve this, total three models were constructed.

The models differed in their shear reinforcement at the joint. One model was constructed with tie and another without tie at the joint as control specimen. The other model was constructed without any tie at the joint but retrofitted with CFRP.

Exterior joints are subjected to high shear force under cyclic loading and may fail if the shear strength of the joint is insufficient to resist the induced shear force. The conventional methods of retrofitting found to be structurally effective but cause rehabilitation, aesthetic degradation and time consuming. FRP found to be very effective in restoring and improving shear and flexural capacity of the existing structures and have been recommended by numerous scholars. BC joints are difficult to access therefore they are also difficult to retrofit by conventional methods. Efforts are taken to retrofit the exterior beam column joints by CFRP and investigate their behavior.

The models were constructed in single phases from the same batch of fresh concrete to obtain identical strengths and properties. Existing construction practices in pre and post construction phases were also followed so that the test results are compatible for practical purpose. The joint of test sample was retrofitted by CFRP Fabrics by following the standard procedure and manuals provided by the manufacturer.

Three dial gauges were fixed to measure the deflection of beams and columns under cyclic loading. Cyclic loading and the corresponding deflections were manually recorded. Joint rotations of the models were recorded by video extensometer against time by the computer. Times corresponding to particular load were manually recorded to relate load Vs rotation.

Load-deflection curve of beam and columns and M-Φ curve of the joints are plotted to study their behavior under cyclic loading. Each cycle of the load deflection and M-Φ

curve are analyzed to justify the behavior of the beams and columns in general and the exterior joints in particular. Conclusions are drawn basing on the qualitative analysis and experimental results.

6.2 Conclusion

Behavior of the exterior joints under cyclic loading, both of the control specimens and the retrofitted ones, were investigated based on the performed test result. Following conclusions are drawn based on the experiment and analysis of the results:

a. Shear stress required for joint failure cannot be reached as flexural failure of beam initiated.

b. The effect of shear reinforcement at joint was not found because the joint failure did not initiate.

c. Rotational stiffness of the retrofitted joints was higher than that of the control models.

d. The stiffness of the joints decreased gradually under cyclic loading. But, Stiffness of FRP retrofitted joint degraded relatively slowly than that of control models.

e. The rotational ductility of the joints increased 8.58% by strengthening the BC joints with FRP.

f. The energy absorption capacity of joint increased 21% by the use of FRP.

6.3 Recommendations for Further Study

a. To investigate the effect of shear reinforcement at joint the test can be repeated by reducing column size and concrete strength

b. The experimental results may be verified by finite element analysis.

c. The study may be conducted on more number of full scale models with strain gauge and actuators.

d. Joints strengthened by CFRP Plate and Fabrics together may be investigated.

e. Parametric study of all the strengthened joints may be conducted for design rationale.

f. The change in lateral load carrying capacity of a multistoried frame structure building by the use of FRP can be analyzed.

REFERENCES:

ACI353R-02. (2002). "Recommendation for Design of Beam-Column Connections in Monolithic Reinforced Concrete Structure." reported by ACI Committee 352.

ACI 440.2r-08. (2008). "Guide for the Design and Construction of Externally Bonded FRP Systems for Strengthening Concrete Structures," reported by ACI Committee 440.

ACI 440.2r-02. (2002). "Guide for the Design and Construction of Externally Bonded FRP Systems for Strengthening Concrete Structures," reported by ACI Committee 440.

Almusallam, Tarik H., and Al Salloum., Yousef . (2007). "Seismic Response of Interior RC Beam-Column Joints Upgraded with FRP Sheets. I: Experimental Study." ASCE Journal of Composites For Construction., Vol 11, No 06, Nov-Dec, pp 575-589.

Al-Salloum, Y.A., Alsayed, S. H., Almusallam, T. H., and N. A. Siddiqui. (2007)."Seismic Response of Interior RC Beam-Column Joints Upgraded with FRP Sheets. II: Analysis and Parametric Study." ASCE, Journal of Composites for Construction., vol. 11, No 6, pp 301-311.

Akguzel,U., and Pampanin, S. (2007). "Seismic Response of RC Beam-Column Joints Upgraded with FRP Sheets. II: Analysis and Parametric Study." ASCE, Journal of Composites for Construction, Vol. 11, No 6, pp. 590-600.

Akguzel,U., and Pampanin, S. (2008). "Effects of Variation of Axial Load and Bi-Directional Loading on the FRP Retrofit of Existing B-C Joints." presented at 14th World Conference on Earthquake Engineering, Beijing, China, October 12-17.

Akguzel, U., and Pampanin, S. (2012). "Assessment and Design Procedure for the Seismic Retrofit of Reinforced Concrete Beam-Column Joints using FRP Composite Materials." ASCE, Journal of Composites for Construction, Vol. 16, No 1, pp. 21-34.

Bai, Jong Wha., (2003). "Seismic Retrofit for Reinforced Concrete Building Structures." Consequence Based Engineering (CBE) Institute Final Report., Mid-America Earthquake Center.

Costas P. Antonopoulos and Thanasis C. Triantafillou,

Experimental Investigation of FRP-Strengthened RC Beam-Column Joints

J. Composites Construction / FEBRUARY 2003 / 39

Castellani, A., Negro, P., Colombo, A., Grandi, A., Ghisalberti, G., and Castellani, M. (1999) ''Carbon fiber reinforced polymers (CFRP) for strengthening and repairing under seismic actions.''

Special Publication No. I.99.41, European Laboratory for Structural Assessment, Joint Research Center, Ispra, Italy.

Cheung, P.C., Paulay, T., and Park, R. (1991). "Mechanisms of Slab Contributions in Beam Column Sub assemblages, Design of Beam-Column Joints for Seismic Resistance." SP-123, American Concrete Institute, Farmington Hills, Mich., pp.259-289.

Cosgun, Cumhur., Comert, Mustafa., Demeir, Cem., and Ilki, Alper. (2012). " FRP Retrofit of a Full Scale 3D RC Frame," Istanbul Technical University.

Dhakal, R.P., Pan, T.C. and Tsai, K.C. (2003). "Enhancement of Beam-Column Joint by RC Jacketing," online citation http://hdl.handle.net/10092/4198.

Ehsani, M. R. (1993). "Glass-Fiber Reinforcing Bars, Alternative Materials for the Reinforcement and Prestressing of Concrete," J.L. Clarke, Blackie Academic & Professional, London, England, pp. 35-54.

Engindniz , Murat., Lawrence, F Kahn., and Zureick, Abdul Hamid. (2005). " Repair Strengthening of Reinforced Concrete Beam Column Joints: State of Art." Structural Journal, ACI , vol 102, No 02, pp 1015.

Federal Emergency Management Agency (FEMA). (1997). "NEHRP Guidelines for Seismic Rehabilitation of Buildings October." FEMA 273.

Gergely, J., Pantelides, C. P., and Reaveley, L. D. (2000).

''Shear strengthening of RC T-Joints using CFRP composites.''

J. Composite Construction, 4(2), (56–64).

Geng, Z.-J., Chajes, M. J., Chou, T.-W., and Pan, D. Y.-C. (1998).

''The retrofitting of reinforced concrete column-to-beam connections.''

Compos. Sci. Technol., 58, 1297–1305.

Hakuto, S., Park, R., and Tanaka, H. (2000). "Seismic Load Tests on Interior and Exterior Beam-Column Joints with Substandard Reinforcing Details." Structural journal, ACI, 97(1), pp11-25.

Ichinose, T. (1991). "Interaction between Bond at Beam Bars and Shear Reinforcement in RC Interior Joints, Design of Beam-Column Joints for Seismic Resistance." SP-123, American Concrete Institute, Farmington Hills, Mich., pp. 379-400.

ILki, Alper., Bedirhangolu, Idris., and Kumbasa, Nadir., (2011). "Behavior of FRP-Retrofitted Joints Built with Plain Bars and Low Strength Concrete." Journal of Composite Construction, ASCE, vol.15, No 3, pp 312-326.

Joh., Osamu., Goto Yasuaki. (2000). "Beam Column Joint Behavior after Beam Yielding in R/C Ductile Frames." paper presented on 12 WCEE Conference, Auckland, New Zealand., 30January-04 February.

Kibria, B. M. Golam. (2014). "Experimental Investigation on Behavior of Reinforced Concrete (RC) Interior Beam Column Joints Retrofitted with Fiber Reinforced Polymers (FRP)." M. Sc. thesis paper, Department of Civil Engineering, Bangladesh University of Engineering & Technology (BUET), Dhaka.

Li, Bing., and Qi, Qiang. (2011). "Seismic Behavior of the Reinforced Concrete Interior Beam-Wide Column Joints Repaired using FRP." Journals of Composites for Construction, ASCE, May-June, vol 15, No 3, , pp 327-338.

Li, Bing., Kai, Qian., and Thanh, Cao Ngoc Tran. (2013). "Retrofitting Earthquake Damaged RC Structural Walls with Openings by Externally Bonded FRP Strips and Sheets." Journal of Composites for Construction, ASCE, Vol. 17, No 2, pp. 259-270.

Lakshmanan, N. (2006). "Seismic Evaluation and Retrofitting of Buildings and Structures" Journal of Earthquake Technology, ISET, Vol. 43, No 1-2, pp 31-48

Leon, R.T. (1990). "Shear Strength and Hysteretic Behaviour of Beam-Column Joints," ACI Structural Journal, Jan-Feb, vol.87, No.1, pp. 3-11

Mahini, SS., and Ronagh, H.R. (2007). "A New Method For Improving Ductility in Existing RC Ordinary Moment Resisting Frames using FRPs." Asian Journal of Civil Engineering (Building and Housing), vol.8, No.6, pp 581-595.

Mayfield, B., Kong, K.F. and Bennison, A. (1971). "Corner joint details in structural light weight concrete"., ACI journal, May, Vol. 65, No.5, pp. 366-372.

Mosallam, A. (1999).

"Seismic repair and upgrade of structural capacity of reinforced concrete connections: Another opportunity for polymer composites."

Proc., Int. Composites Expo '99, Cincinnati, 1-8.

Mutsuyoshi, H., Uehara, K., and Machida, A. (1990) "Mechanical Properties and Design Method of Concrete Beams Reinforced with Carbon Fiber Reinforced Plastics." Transaction of the Japan Concrete Institute, vol. 12, Japan Concrete Institute, Tokyo, Japan, pp. 231-238.

Mukharjee, Abhijeet., and Joshi., Mangesh., (2005). "FRPC Reinforced Concrete Beam-Column Joints under Cyclic Excitation." Journal of Composite Structure, 70 (02) pp 185-199.

Murshed, Arefin., and Ahmed, Ishtiaque., (2011). " Seismic Performance of Soft Storey Structures Retrofitted with FRP Wraps." MSc Thesis Paper., Bangladesh University of Engineering and Technology.

Neville, A.M. (1995) " Properties of Concrete," chap 3, pp 108-120, 4th Edition, Pearson Education, Inc, Nodia, India.

Nilson., H Arthur. (1997). "Design of Concrete Structures." 12 Edition, chap 10, pp 332-358, The McGraw-Hill Companies, Inc, New York.

NPTEL -Module 16, Lesson 40, "Ductile Design and Detailing of Earthquake Resistant Structures." retrieved from ww.nptel.ac.in/courses/105105104/pdf/m16l40.pdf

Paulay, T. and Priestley, M.J.N. (1992). "Seismic Design of Reinforced Concrete and Masonry Buildings." John Wiley Publications, New York.

Prota, Andreas., Nanni , Anotnia., Gaetano, Manfredi., and Cosenza, Edoward. (2004). "Selective upgrade of under Designed Reinforced Concrete Beam-Column Joints Using Carbon Fiber Reinforced Polymers." ACI Structural Journal, Sep-Oct vol 101, No 5, pp 699-707.

Prince Engineering, "FRP Reinforcement for Structures" retrived from www.build-on-prince.com/frp-reinforcement.html#sthash.BKNnh1hT.dpbs

Pantelides, P Chris., Clyde Chandra., and Dreaveley, Lawrence. (2000). "Rehabilitation of R/C Building Joints with FRP Composites." paper presented on 12 WCEE Conference, Auckland, New Zealand., 30January-04 February.

Pampanin, S., Calvi, G M., and Moratti, M.. (2002). "Seismic Behaviour of R.C. Beam-Column Joints Designed for Gravity Loads." paper presented on 12th European Conference on Earthquake Engineering., 9-13 September , London.

Paulay, T., and Priestley, M.J.N. (1992). "Seismic Design of Reinforced Concrete and Masonry Buildings," John Wiley publications New York.

Shiohara, Hitoshi., and Kusiara, Fumio. (2010). "An Overlooked Failure Mechanism of Reinforced Concrete Beam-Column Joints," proceedings of the 9th U.S. National and 10th Canadian Conference on Earthquake Engineering, July 25-29, Toronto, Ontario, Canada.

Sezen, Halil. (2012). "Repair and Strengthening of Reinforced Concrete Beam-Column Joints with Fiber Reinforced Polymer Composites." Journal of Composites for Construction, ASCE, vol. 16, No 5 pp 499-506.

Shannag, M.J., Barakat, S. and Abdul-Kareem, M. (2002). "Cyclic Behavior of HPFRC-Repaired Reinforced Concrete Interior Beam-Column Joints." Materials and Structures, vol. 35, 348-356.,

Sharma, Akanshu., Gension, G., Reddy, GR., Eligehousen , R., Pampanin, S., and Vaze., KK. (2010). "Experimental Investigations on Seismic Retrofitting of Reinforced Concrete Beam-column Joints." paper ref A007, presented on 14th Symposium on Earthquake Engineering, Indian Institute of Technology, Roorkee, December 17-19.

Standrards New Zealand (NZS). (1995). NZS 3101:1995."New Zealand Concrete Stanadard."

Takiguchi, Katsuki., Abdullah., (2000). "Experimental Study on Reinforced Concrete Beam Strengthened with Ferocement Jacket." paper presented on 12 WCEE Conference, Auckland, New Zealand., 30January-04 February.

Thermou, G. and Elnashai, A.S. (2002). "Performance Parameters and Criteria for Assessment and Rehabilitation." Seismic Performance Evaluation and Retrofit of Structures (SPEAR), European Earthquake Engineering Research Network Report, Imperial College, UK.

Tsonos, A. D., and Stylianidis, K. A. (1999)

''Pre-seismic and post-seismic strengthening of reinforced concrete structural subassemblages using composite materials (FRP).''

Proc., 13th Hellenic Concrete Conference., Rethymno, Greece, 1, 455–466.

Tsonos, A.G. (2000). "Lateral load response of strengthened reinforced concrete Beam-to-column joints," paper presented on 12 WCEE Conference, Auckland, New Zealand, 30January-04 February.

Uma, S.R., and Prasad, A.Meher., (2006). "Seismic Behavior of Beam Column Joints in Reinforced Concrete Moment Resisting Frames." document no IITK-GSDMA-EQ-31-V1-0, IITK-GSDMA Project on Building Code.

Vasani, P.C., Mehta, B Bhumika., "Ductility Requirements for Buildings," retrieved from http://www.sefindia.org/?q=system/files/Ductility-1.pdf.

Wang, Yung-Ching., and Gin Ming., (2004). "Rehabilitation of Non-ductile Beam-Column Joint using Concrete Jacketing," presented at 13th World Conference on Earthquake Engineering, Vacouver, Canada August 1-6.

Wu, W., (1990). "Thermomechanical Properties of Fiber Reinforced Plastics (FRP) Bars." PhD dissertation, West Virginia University, Morgantown, W.Va., 292 pp.

Xiaobing, Song., Xianglin, Go., Li Yupeng., Tao., Chang., and Zhang Weiping. (2013). "Mechanical Behavior of FRP-Strengthened Concrete Columns Subjected to Concentric and Eccentric Compression Loading." Journal of Composite Construction, ASCE, May-June, pp 336-346.

APPENDIX A

Table A.1: Sieve Analysis Report of Sand

Sieve No	Sieve Size (mm)	Weight retained (gm)	Cumulative weight retained (gm)	Cumulative % weight retained	% passing
4	4.75	0.0	0.0	0.0	100
8	2.36	23.5	23.5	4.7	95.3
16	1.19	89.2	112.7	22.5	77.5
30	0.6	162.1	274.8	55.0	45.0
50	0.3	129.6	404.4	80.9	19.1
100	0.15	66.5	470.9	94.2	5.8
Pan	0	29.1	500	-	
Total		500		257.3	

Fineness Modulus (F.M.) =2.57

A.1 CONCRETE MIX DESIGN

Using Software: http://concrete.union.edu/WtSINon.htm/Concrete Mix Design - Design Procedure.htm

Design method: ACI Method (ACI 211.1-91, Reapproved 2002)
Type of concrete: NON-AIR-ENTRAINED

1) SLUMP

Table A.2: Recommended slumps for various types of construction

Types of construction	Maximum Slump (in.)	Minimum Slump (in.)
Reinforced foundation walls and footings	3	1
Plain footings, caissons, and substructure walls	3	1
Beams and reinforced walls	4	1
Building columns	4	1
Pavements and slabs	3	1
Mass concrete	2	1

From Table above slump values are:

Maximum = 4 in;   Minimum = 1 in.

2) MAXIMUM AGGREGATE SIZE
The nominal maximum size of coarse aggregate = 3/4 in.

3) MIXING WATER & AIR CONTENT

Table A.3: Approximate mixing water (lb/yd³) for indicated nominal maximum sizes of aggregate

AIR-ENTRAINED CONCRETE								
Slump (in.)	3/8 in.	1/2 in.	3/4 in.	1 in.	1 1/2 in.	2 in.	3 in.	6 in.
1 to 2	350	335	315	300	275	260	220	190
3 to 4	385	365	340	325	300	285	245	210
6 to 7	410	385	360	340	315	300	270	-
Air Content	3%	2.5%	2%	1.5%	1%	0.5%	0.3%	0.2%

From Table above, the water weight for non-air-entrained concrete = [340] lb/yd³
And the amount of entrapped air = [2] %

4) WATER-CEMENT RATIO

Table A.4: Relationship between water-cement or water-cementitious materials ratio and compressive strength of concrete

28 day Compressive strength (psi)	Water-cement ratio, by weight	
	Non-air-entrained concrete	Air-entrained concrete
7000	0.33	--
6000	0.41	0.32
5000	0.48	0.40
4000	0.57	0.48
3000	0.68	0.59
2000	0.82	0.74

Required compressive strength at 28 days = [3500] psi

Water-cement (or water-cementitious materials) ratio (from Table above) = [0.625]

Important! It should be checked the maximum permissible water-cement ratio from the Table below and revise the water-cement ratio entered in the box above accordingly.

Table A.5: Maximum permissible water-cement or water-cementitious materials ratios for concrete in severe exposure

Type of Structure	Structure wet continuously and exposed to frequent freezing and thawing	Structure exposed to sea water or sulfates
Thin section (railings, curbs, sills, ledges, ornamental work) and sections with less than 1 in. cover over steel	0.45	0.40
All other structures	0.50	0.45

The specific gravity of the cement (if unknown, use 3.15) = $\boxed{3.15}$

Weight of cement = $\dfrac{340}{0.625} = 544\,\dfrac{lb}{yd^3}$ $\boxed{544}$ lb/ft

5) COARSE AGGREGATE

Table A.6: Volume of coarse aggregate per unit of volume of concrete

Nominal maximum size of aggregate (in.)	Volume of oven-dry-rodded coarse aggregate per unit volume of concrete for different fineness moduli of fine aggregate			
	2.40	2.60	2.80	3.00
$^3/_8$	0.50	0.48	0.46	0.44
$^1/_2$	0.59	0.57	0.55	0.53
3/4	0.66	0.64	0.62	0.60
1	0.71	0.69	0.67	0.65
$1^1/_2$	0.75	0.73	0.71	0.69
2	0.78	0.76	0.74	0.72
3	0.82	0.80	0.78	0.76
6	0.87	0.85	0.83	0.81

Nominal maximum size of aggregate is $\boxed{3/4}$ in.

The unit weight of coarse aggregate (if unknown, use 95 to 120 lb/ft^3 for normal weight aggregate) = $\boxed{95}$ lb/ft^3

The fineness modulus of fine aggregate (from Table A.1) = [2.57]

From Table above, volume of coarse aggregate per unit volume of concrete = [0.643]

Enter specific gravity of coarse aggregate (if unknown, use 2.55 to 2.75 for normal weight aggregate) = [2.65]

Oven dry Weight of coarse aggregate = 0.643 x 27 ft^3/yd^3 x 95 = [1649.3] lb/yd^3

6) FINE AGGREGATE

Estimation of fine aggregate content by the absolute volume method:

⇌ Water:	340 lb./62.4 lb./ft.^{3}	= 5.49 ft.^{3}
⇌ Cement:	544 lb./(3.15 x 62.4 lb./ft.^{3})	= 2.76 ft.^{3}
⇌ Coarse Aggregate:	1649.3 lb./(2.65 x 62.4 lb./ft^3)	= 9.97 ft^3
⇌ Air:	2% x 27ft^3/yd^3	= 0.54 ft.^{3}

$$\text{Total} = 18.76 \text{ ft}^3$$

The specific gravity of fine aggregate (if unknown, use 2.55 to 2.75 for normal weight aggregate) = [2.63]

Fine Aggregate occupies the volume of: 27 ft.^{3} -18.76 ft.^{3} = 8.24 ft.^{3}

The Oven Dry Weight of fine aggregate =8.24 ft.^{3} x2.63x 62.4 lb/ft^3 = [1352.3] lb/yd^3

7) ADJUSTMENT FOR MOISTURE IN AGGREGATE

Design mix water = [340] lb/yd^3

Total moisture content in coarse aggregate = [0.4] %

The absorption capacity of coarse aggregate = [3.1] %

Total moisture content in fine aggregate = [4] %

The absorption capacity of fine aggregate = [2.4] %

Net mix water =340-1649 x(0.004-0.031) -1352.3 x(0.04 -0.024) = [362.8] lb/yd^3

The SSD Weight of coarse aggregate = 1649.3 lb/yd^3 x 1.031 = [1700.4] lb/yd^3

The SSD weight of fine aggregate =1352.3 lb/yd^3 x 1.04 = [1406.3] lb/yd^3

8) SUMMARY OF MIX DESIGN

Batch percentage (for 50 kg of cement) = [20.2] %

Compressive strength at 28 days = [3500] psi

Slump:

Maximum = [4] in &   Minimum = [1] in.

Nominal maximum size of aggregate = [3/4] in.

Water-cement (or water-cementitious materials) ratio = [0.625]

Concrete type is [Non-Air-entrained]

Air content = [2] %

Unit weight of coarse aggregate = [95] lb/ft^3

Ingredients of Concrete Mixture:

Water lb/yd^3	Cement lb/yd^3	Coarse Aggregate lb/yd^3	Fine Aggregate lb/yd^3
362.4	544	1700.4	1406.3

Ingredients of [20.2] **% Concrete Batch:**

Water (kg)	Cement (kg)	Coarse Aggregate (kg)	Fine Aggregate (kg)
33.2	50.0	155.8	128.8

Table A.7: Cylinder Strength Test Result (28th days):

Sample	Dia (mm)	Cross Sectional Area (mm^2)	Applied Load (kN)	Strength (MPa)	Average Strength (MPa)
S-1	101.2	8043	310	38.5	
S-2	102.0	8171	311	38.06	38.42
S-3	101.8	8139	315	38.7	

APPENDIX B

Table B.1: Load vs. Displacement of Beam

Sample No	Cycle	Forward Cycle		Reverse Cycle	
		Applied Load (kN)	Maximum Displacement (mm)	Applied Load (kN)	Maximum Displacement (mm)
Model-C1	Cycle-I	11.07	5.3	-8.85	-5.7
	Cycle-II	14.76	8.3	-29.52	-20.7
	Cycle-III	22.14	30.3	-29.52	-29.7
	Cycle-IV	18.45	45.3	-25.83	-32.7
Model-C2	Cycle-I	17.32	9	-17.325	-8
	Cycle-II	27.72	19.5	-24.25	-14
	Cycle-III	31.185	27	-29.1	-28
	Cycle-IV	27.72	38	-31.185	-43
Model-F	Cycle-I	17.325	5.7	-20.79	-8
	Cycle-II	20.79	8.7	-31.185	-19.3
	Cycle-III	24.25	17.7	-31.185	-27.3
	Cycle-IV	27.72	26.7	-31.185	-33.33
	Cycle-V	27.72	40.9		

Table B.2: Load vs. Displacement of Column

Sample No	Cycle	Forward Loading		Reverse Loading	
		Column Shear (kN)	Maximum Displacement (mm)	Column Shear (kN)	Maximum Displacement (mm)
Model-C1	Cycle-I	10.53	1.4	-8.42	-0.95
	Cycle-II	14.04	2.4	-28.07	-4.45
	Cycle-III	21.06	4.67	-28.07	-5.29
	Cycle-IV	17.55	5.03	-21.05	-6.34
Model-C2	Cycle-I	16.47	1.8	-16.48	-2.2
	Cycle-II	26.36	2.9	-23.07	-3.9
	Cycle-III	29.65	3.7	-27.68	-4.8
	Cycle-IV	26.36	3.6	-29.66	-5.9
	Cycle-V	26.36	3.9	-29.65	-6.3
Model-F	Cycle-I	16.48	1.5	-19.77	-2.1
	Cycle-II	19.77	2.0	-29.66	-4.9
	Cycle-III	23.07	2.4	-29.66	-7.2
	Cycle-IV	26.36	2.0	-29.66	-7.9
	Cycle-V	29.66	3.3	-32.95	-8.3

Table B.3: Moment vs. Rotation (M-Φ) of Joints

Sample No	Cycle	Forward Cycle			Reverse Cycle		
		Applied Moment (kN-m)	Maximum Beam Joint Rotation (Degree)	Maximum Column Joint Rotation (Degree)	Applied Moment (KN-m)	Maximum Beam Joint Rotation (Degree)	Maximum Column Joint Rotation (Degree)
Model-C2	Cycle-I	21	0.112	0.132	-21	-0.164	-0.147
	Cycle-II	33.6	0.218	0.256	-29.4	-0.251	-0.257
	Cycle-III	37.8	0.265	0.311	-35.28	-0.321	-0.334
	Cycle-IV	33.6	0.245	0.296	-37.8	-0.364	-0.406
	Cycle-V	33.6	0.257	0.298	-37.8	-0.364	-0.403
Model-F	Cycle-I	21	0.043	0.066	-25.2	-0.177	-0.168
	Cycle-II	25.2	0.1306	0.0885	-37.8	-0.402	-0.395
	Cycle-III	29.4	0.131	0.1302	-37.8	-0.491	-0.469
	Cycle-IV	33.6	0.086	0.1046	-37.8	-0.53	-0.511
	Cycle-V	33.6	0.102	0.149	-42	-0.552	-0.534

Table B.4: Energy Absorption of Joint

Sample No	Cycle	Energy Absorption		
		Forward Loading (kN-m)	Reverse Loading (kN-m)	Total (kN-m)
Model-C1	Cycle-I	3.65	10.33	1371.35
	Cycle-II	27.30	135.05	
	Cycle-III	314.57	407.74	
	Cycle-IV	366.23	500.0	
Model-C2	Cycle-I	8.66	19.05	3047.05
	Cycle-II	165.62	168.05	
	Cycle-III	469.5	544.0	
	Cycle-IV	648.93	1023.2	
	Cycle-V	1258.54	-	
Model-F	Cycle-I	16.63	55.44	3697.6
	Cycle-II	103.95	198.37	
	Cycle-III	294.18	378.72	
	Cycle-IV	442.48	630.63	
	Cycle-V	1557.19	-	

Table B.5: Stiffness of Beam

Sample No	Cycle	Stiffness		
		Forward Loading (kN-m)	Reverse Loading (kN-m)	Maximum Value (kN-m)
Model-C1	Cycle-I	2.089	1.155	2.089
	Cycle-II	1.778	1.426	1.778
	Cycle-III	0.731	0.993	0.993
	Cycle-IV	0.407	0.677	0.677
Model-C2	Cycle-I	1.925	2.166	2.166
	Cycle-II	1.422	1.733	1.733
	Cycle-III	1.155	1.040	1.155
	Cycle-IV	0.729	0.725	0.729
Model-F	Cycle-I	3.039	2.505	3.039
	Cycle-II	2.390	1.616	2.390
	Cycle-III	1.370	1.142	1.370
	Cycle-IV	1.038	0.936	1.038

B.1 Plastic Yield Moment of the Joint

According to ACI Committee recommendation Ultimate plastic moment strength of the joint is calculated based on the nominal strength of the members. As the beam is designed as under-reinforced one, the tension force from negative reinforcement is to be taken as

$$T = Asfy \; ;$$

And the compression force from equilibrium is

C = T;

Then the ultimate moment capacity at the joint is

$$Mu = T\left(d - \frac{a}{2}\right)$$ ....(B.1)

Where 'a' is the stress block depth computed as $a = \dfrac{C}{.85fc'b}$.

Calculated plastic moment capacity of the beams of all the samples before strengthening the joints are shown through Table B.6.

Table B.6: Plastic Moment Strength of Beams

Model No	As (mm^2)	f´c (MPa)	fy (MPa)	T_{ult} (kN)	a (mm)	$d - \dfrac{a}{2}$ (mm)	M_u (kN-mm)	P_{ult} (kN)
Model-C1	207	38.42	500	103.5	21	183.5	18992.3	15.65
Model-C2	207	38.42	500	103.5	21	183.5	18992.3	15.65
Model-F	207	38.42	500	103.5	21	183.5	18992.3	15.65

L=1213 mm, d=194 mm, b=150 mm.

B.2 Shear strength capacity of the Joint

The nominal shear strength of a joint is given by the equation

$$V_n = \gamma \sqrt{f_c'} b_j h$$

Where b_j is the effective joint width in inches, h is the column thickness in inches in the direction of load being considered. Considering the confinement of the joint the value of γ is found 12. b_j can be calculated as $b_j = \dfrac{b_b + b_c}{2}$ and $b_j \leq b_b + h$, where b_b is the beam width and b_c is the column width. Shear strength capacity of the joint has been calculated for all models in Table B.7.

Table B.7: Shear Strength Capacity of the Joints

Model No	b$_j$ (mm)	f´c (MPa)	h (mm)	V$_n$ (kN)
Model-C1	187.5	38.42	225	260.4
Model-C2	187.5	38.42	225	260.4
Model-F	187.5	38.42	225	260.4

B.3 Design Shear strength of the Joint

According to ACI Committee 352, joint region should be designed based on nominal strength of the members connected at the joint. The design moment applied at the joint face is that corresponding to the moment capacity of the beam M_u and the tension force T as calculated in earlier section B.1 from the equation B.1 in Table B.6. Then the joint shear is given by

$$V_u = T - V_{Col}$$; where V_{Col} is found for exterior joint is $\dfrac{M_u}{Column\ height\ (h_{col})}$.

Table B.8: Maximum Shear Stress Developed at the Joints

| Model No	M_u (kN-mm)	T (kN)	h_{Col} (mm)	V_{Col} (kN)	$V_u = T - V_{Col}$ (kN)
Model-C1	18992.3	103.5	1275	14.9	88.6
Model-C2	18992.3	103.5	1275	14.9	88.6
Model-F	18992.3	103.5	1275	14.9	88.6

Table B.9: Rotational ductility of Joints

Sample No	Maximum rotation		Rotational ductility (Degree)	Increment (%)
	Forward Cycle (Degree)	Reverse Cycle (Degree)		
Model-C2	0.265	0.364	0.629	-
Model-F	0.131	0.552	0.683	8.58

APPENDIX C

STEEL FRAME BUILT FOR THE EXPERIMENT
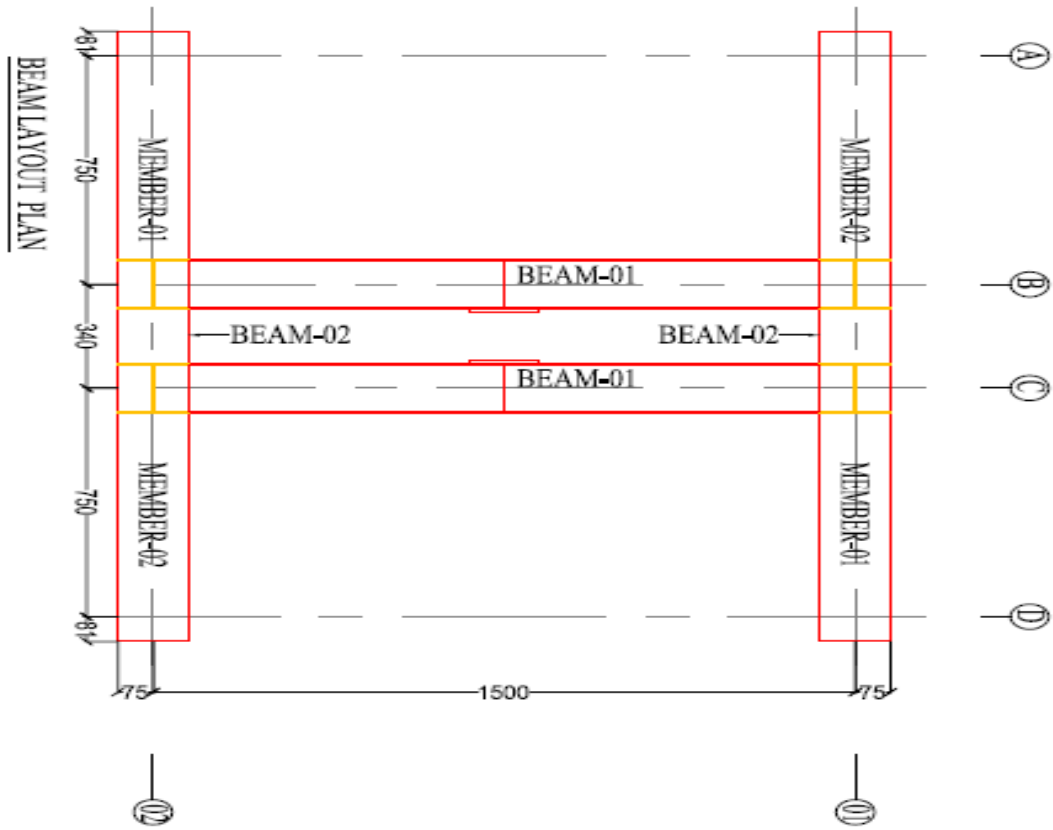
ig. C.1.01: Beam Layout Plan of the Frame
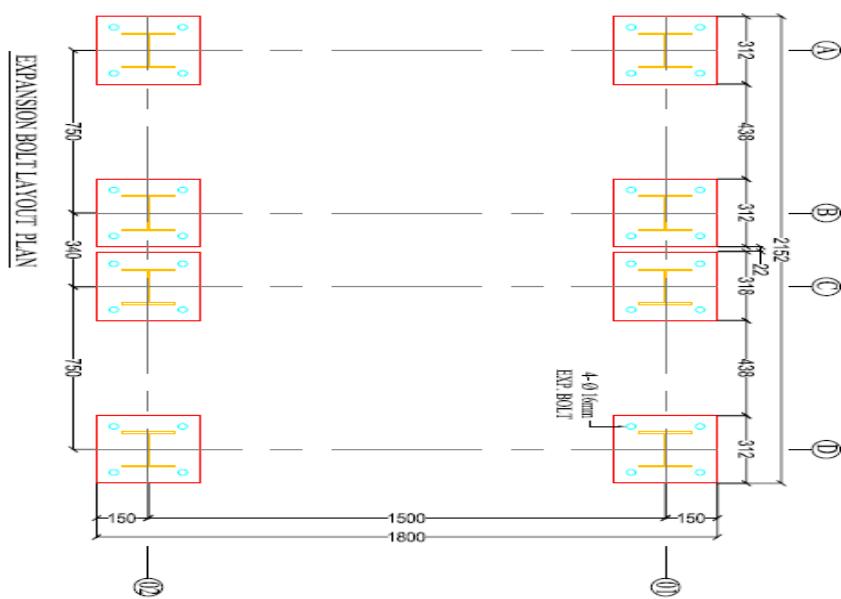
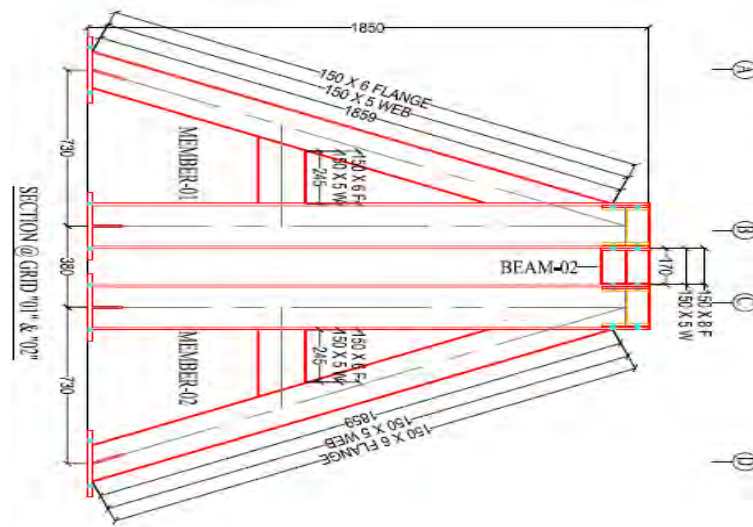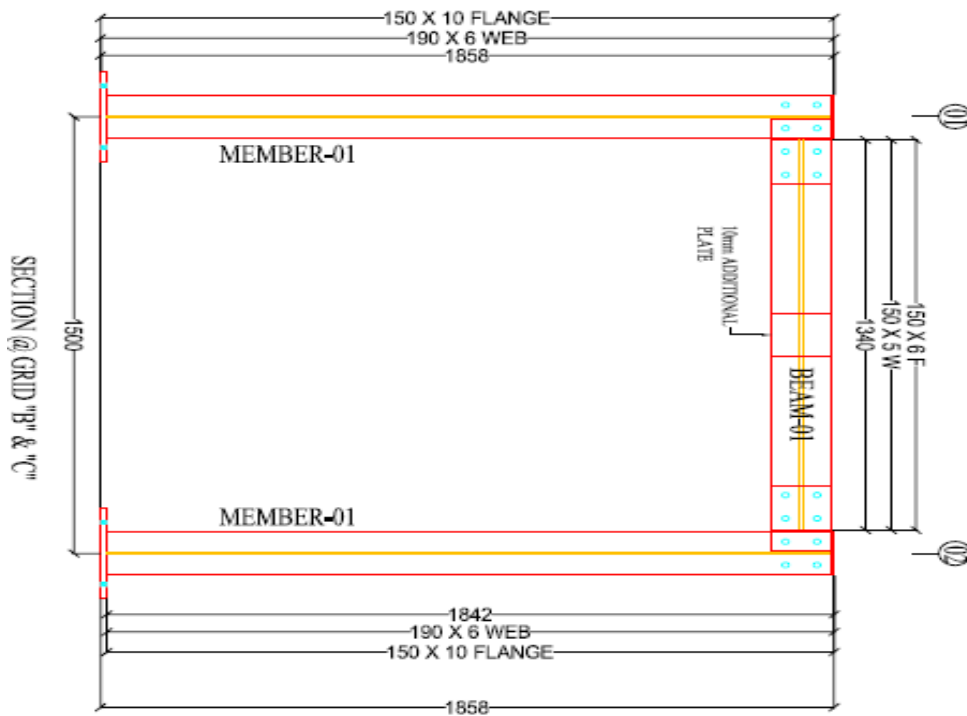**Fig. C.1.02: Expansion Bolt Layout Plan of the Frame**

Fig. C.1.03: Front View of the Frame

Fig. C.1.04: Side View of the Frame